Check for updates



small methods
www.small-methods.com

# Surface Organic Nanostructures Mediated by Extrinsic Components: from Assembly to Reaction

*Chi Zhang,* Rujia Hou, and Wei Xu**

**Surface organic nanostructures demonstrate great potential across multidisciplinary fields ranging from molecular electronics to energy conversion and storage. In the regime of surface chemistry, their preparation generally relies on intrinsic components originally involved in the molecule-substrate systems to drive molecular assembly and reaction. The recent paradigm shift employs extrinsic components as functional mediators to precisely regulate nanostructure formation pathways and the resulting molecular nanostructures. This review highlights three categories of extrinsic modulators, including small gas molecules, metals, and their combinations, that allow the construction and modification of surface organic nanostructures through tailored assembly and reaction. In addition, their detailed roles and regulatory mechanisms at the single-molecule level are also discussed. This emerging extrinsic-components-mediated assembly and reaction methodology displayed herein enriches the preparation toolbox for surface organic nanostructures and further allows the modification of their physicochemical properties, opening new frontiers in supramolecular engineering, nanomaterials development, etc.**

## 1. Introduction

With the increasing demand for electronic components, the realization of miniaturization of electronic devices is an urgent trend. Since the mid-1970s, the idea of embedding single or multiple molecules between electrodes to realize the basic functions of digital electronics, including rectification, amplification, and storage, has been proposed,[1] and a great deal of relevant research has been carried out. Various organic functional structures have been demonstrated to be available for the construction of electronic components, such as molecular switches, molecular wires, molecular memory devices, etc. Therefore, the construction of electronic devices based on functional single molecules and molecular nanostructures is expected to be one of the feasible ways to solve the ultimate miniaturization.[1,2] Among others, the utilization of single molecules to realize basic electronic functions has gained tremendous research progress, such as molecular wires composed of $\pi$-conjugated molecular oligomers[3] and molecular optical memories, switches and actuators composed of photochromic molecules.[4] Furthermore, based on the primary functions of single molecules, it has become a new challenge to form well-ordered arrangements of functional organic molecules and further establish efficient and stable electron transport, thus realizing complete functionalized circuits at the molecular scale.

To probe molecular arrangements and intermolecular interactions at the submolecular level, surface science techniques have been generally employed. For examples, scanning tunneling microscopy (STM) resolves topographic skeletons with atomic precision. Atomic force microscopy (AFM) directly measures interaction forces between molecules. Meanwhile, X-ray photoelectron spectroscopy (XPS) deciphers chemical environmental signatures. These complementary methods collectively offer multidimensional insights into both structural configurations and chemical states. In particular, the ultrahigh vacuum (UHV) experimental environment eliminates atmospheric and contaminant interferences and ensures clean characterization conditions for model systems. On these bases, organic molecules, metal atoms, and other components are deposited as building blocks on atomically flat substrates, forming target molecular systems. These molecular systems are ideal for exploring and regulating molecular arrangements, and for elucidating the roles that all kinds of intermolecular interactions and molecule-substrate interactions play in these arrangements. Such a research field is thus classified as molecular assembly on surfaces,[5–7] which deals with noncovalent interactions and provides fundamental understanding for the conceiving and fabrication of functional molecular nanostructures.

The 21st century ushered in great progress in surface science and technology. Building upon molecular assembly, Grill's team achieved a conceptual revolution in their 2007 landmark study,[8] i.e., on-surface synthesis. It takes advantage of molecular building blocks (i.e., precursors) with strategically designed reactive moieties that undergo controlled activation by external stimuli, thereby forming stable covalent connections between molecular units in a bottom-up manner. The resulting covalent nanos-

C. Zhang, R. Hou, W. Xu
Interdisciplinary Materials Research Center
School of Materials Science and Engineering
Tongji University
Shanghai 201804, P. R. China
E-mail: zhangchi11@tongji.edu.cn; xuwei@tongji.edu.cn

The ORCID identification number(s) for the author(s) of this article can be found under https://doi.org/10.1002/smtd.202402118

**DOI: 10.1002/smtd.202402118**

 © 2025 Wiley-VCH GmbH

tructures exhibit enhanced electron transport efficiency between units and structural stability.[8–10] This programmable approach establishes a reliable framework for constructing intermolecular covalent architectures. Moreover, the introduction of solid surfaces provides dual functionality. First, they provide well-defined platforms for some classical solution-based reactions[8–10] (e.g., Ullmann coupling reactions). Second, molecule-surface interactions overcome inherent constraints of traditional solution chemistry through two synergistic mechanisms: i) the catalytic effect, and ii) 2D confinement of the surfaces. This unique combination facilitates surface-catalyzed reactions[11–13] with reduced reaction barriers and establishes unprecedented surface-mediated reaction pathways. In addition, the rational design and modification of molecular precursors allows the optimization of reaction products in terms of structures, dimensions, and properties. Accordingly, low-dimensional functional nanostructures and nanomaterials have been prepared via on-surface reactions, such as conjugated molecular conductors,[10] various graphene nanoribbons (GNRs),[14,15] and porous graphene networks as electrical sensors,[16] etc.

Therefore, by both assembly and reaction strategies, well-controlled arrangement of functional organic molecules into 1D wires, 2D films, or even 3D bulks in the nanometer regime becomes possible. This structural mastery stems from in-depth understanding of the strong relationship between molecular structures and resulting nanostructures.[17] The rapidly developing real-space probing techniques[18] (e.g., STM and AFM) provide powerful tools for investigating molecular assembly and reaction processes on surfaces at the submolecular level. Accordingly, they provide insight into intermolecular interactions and allow for precise characterization of nanostructures and their physicochemical properties.[19,20] In addition, theoretical modeling serves as a computational microscope in surface science. Density functional theory (DFT) calculations decode electronic structures at molecule-substrate interfaces, and molecular dynamics (MD) simulations capture nanoscale assembly or reaction pathways and transition states. These approaches dissect dominant intermolecular interactions and thermodynamic driving forces, and thus bridge electronic behavior with nanoscale phenomena.

Surface nanotechnology has witnessed transformative developments in surface organic nanostructure engineering. Researchers have engineered these architectures through precise manipulation of intrinsic system components. The molecular toolbox principally comprises three elements: i) functional organic building blocks, ii) metallic coordination centers, and iii) underlying crystalline substrates. This tripartite foundation, as demonstrated in prior studies and systematically reviewed elsewhere,[6,7,21–24] generally enables deterministic control over molecular assembly or reaction processes. Recently, an innovative strategy beyond intrinsic system components, that is "extrinsic components", has been successfully introduced into the molecule-substrate systems (as schematically shown in **Figure 1**). Researchers now integrate extrinsic small gas molecules and metal elements (in the form of pure atoms or salts) into molecular assembly and reaction on surfaces. They hold great promise for influencing the components of the molecule-substrate systems, including molecular structures and properties, surface structures and activities, molecule-surface interfacial properties, etc. More specifically, they are expected not only to steer the assembled molecular nanostructures via co-assembly or catassembly,[25] but also to influence the reaction processes by reducing the reaction barriers or temperatures, regulating the reaction pathways, tailoring the reaction products, and so on.

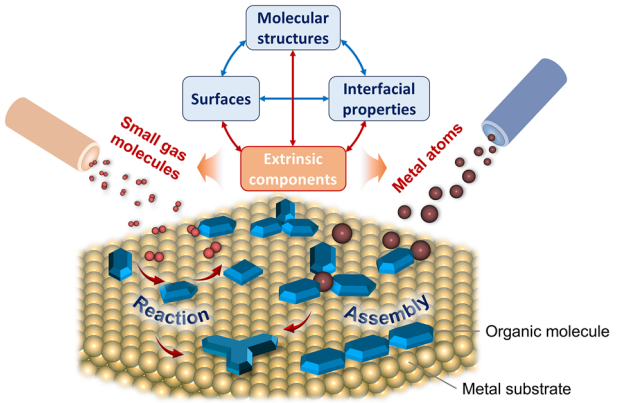


**Figure 1.** Construction of organic nanostructures on surfaces mediated by extrinsic components (mainly including small gas molecules, metal elements, and their combinations in this review) based on molecular assembly and reaction. In such processes, the extrinsic components would influence molecular structures, underlying substrates, and interfacial properties.

In this review, we focus on recent progress in the construction and modification of surface organic nanostructures mediated by extrinsic components via molecular assembly and reaction. A number of typical case studies will be reviewed in terms of different types of extrinsic components, i.e., small gas molecules, metal elements, and their cooperative effects (**Figure 2**). Their roles in facilitating or regulating the assembly and reaction of target organic molecules will also be discussed. In the section of small gas molecules, the application of $H_2O$, CO and $CO_2$, $O_2$ and $H_2$ in the corresponding surface organic nanostructures will be mainly introduced on the basis of several exciting examples (left part of Figure 2). In addition, cases involving extrinsic metals in building corresponding nanostructures will be briefly presented (right part of Figure 2). Moreover, the integration of both small gas molecules and extrinsic metals into surface organic nanostructures and their respective influences will be discussed using our recent example (lower right corner of Figure 2, involving both $O_2$ and Na). Finally, this review will conclude with a brief perspective on the current challenges and future developments in the extrinsic-components-mediated assembly and reaction strategy. The introduction of extrinsic components would enrich the preparation strategies for surface organic nanostructures and assist the modification of their physicochemical properties.

## 2. Small Gas Molecules

Gas molecules, which are widely used in chemical processes such as heterogeneous catalysis, electrochemical catalysis, and metal corrosion, can not only provide the appropriate chemical reaction atmosphere, but also accelerate or regulate the corresponding reaction processes. In heterogeneous catalysis, gas molecules generally undergo a cyclic process of adsorption-reaction-desorption


© 2025 Wiley-VCH GmbH

23669608, 0, Downloaded from https://onlinelibrary.wiley.com/doi/10.1002/smtd.202402118 by Tongji University, Wiley Online Library on [07/04/2025]. See the Terms and Conditions (https://onlinelibrary.wiley.com/terms-and-conditions) on Wiley Online Library for rules of use; OA articles are governed by the applicable Creative Commons License

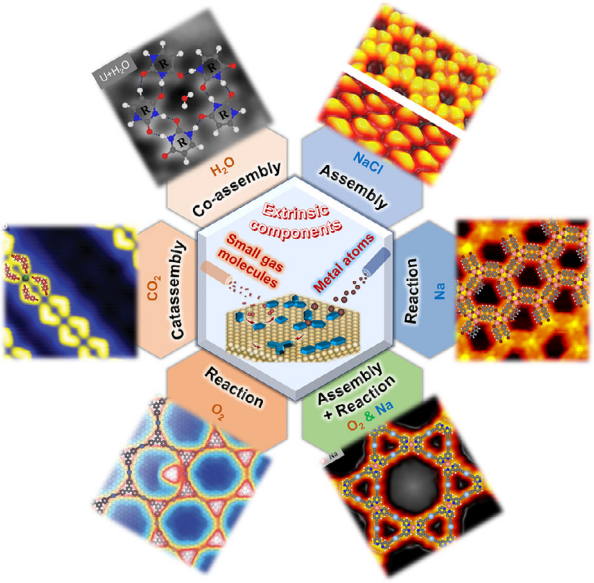


**Figure 2.** Several typical examples of surface organic nanostructures mediated by small gas molecules, metals, as well as their cooperative effects. These images from leftmost to rightmost counterclockwise: Reproduced with permission.[26] Copyright 2021, American Chemical Society. Reproduced with permission.[27] Copyright 2023, Oxford University Press. Reproduced with permission.[28] Copyright 2019, American Chemical Society. Reproduced with permission.[29] Copyright 2024, American Chemical Society. Reproduced with permission.[30] Copyright 2024, American Chemical Society. Reproduced with permission.[31] Copyright 2015, American Chemical Society.

on the surfaces of catalysts, thereby providing a feasible pathway for the selective synthesis of products. In the reactions of electrochemical catalysis and metal corrosion, the adsorption and activation of gas molecules on metal surfaces are also important steps. Their interactions with metal surfaces directly affect the chemical stability and activity of these surfaces.[32,33] In traditional solution chemistry, oxidizing gases, such as $O_2$, are often employed as efficient and sustainable terminal oxidants for various types of C–H activation and C–C coupling reactions.[34,35] In particular, $O_2$ plays an important oxidizing role in the solution synthesis of the unsaturated carbon skeletons of 1,3-diyne via the coupling reactions of terminal alkynes.[36] On the other hand, reducing gases, such as $H_2$, are frequently used as reactants in reactions such as the selective hydrogenation of alkynes to alkenes.[37,38] These above studies suggest that gas-phase engineering emerges as a transformative strategy in molecular reactions on surfaces. Controlled introduction of small gas molecules would potentially allow the modulation of reaction systems by: i) chemically restructuring the microenvironment, ii) electronically modifying metallic substrates or molecule-substrate systems via charge-transfer interactions, and iii) kinetically directing reaction processes. This tripartite control paradigm inspires gas-mediated on-surface synthesis of organic nanostructures. Moreover, some other gas molecules with lower chemical reactivity, such as $CO_2$ and $H_2O$, can assist the assembly processes of target organic molecules with their presence or absence in the eventual nanostructures. Such processes are classified as "co-assembly" and "catassembly" (a new concept proposed by Tian et al.[39] that combines molecular assembly and catalysis), respectively. In these processes, thermodynamic landscapes in gas-mediated molecular assembly are governed by the competition and synergy of intermolecular interactions. The interplay between i) target molecule self-assembly, and ii) target molecules, gas molecules and substrates, dictates two distinct pathways. One is that gas molecules coexist and stabilize the nanostructures with structural transformations. The other is that gas-phase species leave the samples after facilitating structural transitions in response to specific sample temperatures. Especially in the latter case, the gas molecules serve as "catassemblers" that facilitate the processes with high efficiency and/or selectivity and leave, presenting their crucial role in directing organic nanostructures.

In recent years, gas-phase mediation stands as a critical design parameter in surface chemistry. Advanced surface science characterization methods have been extensively applied to understand the preparation of surface organic nanostructures mediated by small gas molecules via molecular assembly and reaction. In the following sections, we will take the applications of some typical gas molecules (i.e., $H_2O$, CO and $CO_2$, $O_2$ and $H_2$) as examples to discuss their influences on the construction and modification of corresponding surface organic nanostructures (also see **Table 1**).

### 2.1. $H_2O$

$H_2O$, as a kind of inert small gas molecule, generally provides hydrogen bonding to some specific functional groups of organic molecules under UHV conditions. As demonstrated in several research papers[40–43] by Morgenstern and co-workers, the dosing of $H_2O$ molecules induced the first steps of hydration[40] and microsolvation[43] processes of organic molecules via co-assembly. Such $H_2O$-involved co-assembly phenomena provide experimental criteria for the direct determination of the molecular conformations as well as the hydrophilic and hydrophobic properties of organic molecules. Moreover, Xu and co-workers have conducted comprehensive studies on $H_2O$-mediated biomolecular assembly on Au(111) through a multidisciplinary approach including high-resolution STM and bond-resolved non-contact AFM (nc-AFM) imaging, single-molecule manipulations, and theoretical calculations.[20,26,44–47] Specifically, the research has focused primarily on DNA and RNA bases—adenine,[44] thymine,[45] guanine,[46] cytosine,[47] and uracil.[26] Notably, in most of these cases, $H_2O$ selectively destroys the weak hydrogen bonding motifs in the assembled organic nanostructures by providing additional hydrogen bonds. It thus leads to the construction of $H_2O$-involved co-assembled structures[44] or the regulation of the original assembled structures,[26,47] while $H_2O$ molecules may eventually be desorbed by further thermal treatment.

Next, we will mainly introduce two detailed cases that demonstrate the influence of $H_2O$ molecules on the surface organic nanostructures from the perspective of both hydration and dehydration.

As schematically illustrated in **Figure 3a**, Xu et al. reported that $H_2O$ molecules (at a pressure of $\approx 8 \times 10^{-5}$ mbar during exposure) are able to efficiently induce the chiral separation


© 2025 Wiley-VCH GmbH

23669608, 0, Downloaded from https://onlinelibrary.wiley.com/doi/10.1002/smtd.202402118 by Tongji University, Wiley Online Library on [07/04/2025]. See the Terms and Conditions (https://onlinelibrary.wiley.com/terms-and-conditions) on Wiley Online Library for rules of use; OA articles are governed by the applicable Creative Commons License

**Table 1.** Summary of the application of some typical small gas molecules in the construction and modification of surface organic nanostructures.

| Gas molecules | Target organic molecules | Substrates | Assembly / reaction | Roles | Refs. |
|---|---|---|---|---|---|
| $H_2O$ ($D_2O$) | 4,4′-hydroxy-azobenzene; 4,4′-dihydroxy-azobenzene; 3-methoxy-9-diazofluorene; 5-(4-nitrophenylazo)salicylic acid | Au(111) | Assembly | Co-assembly (hydration) | [40–43] |
| | adenine; thymine | Au(111) | Assembly | Co-assembly (dynamic hydration, chiral inversion) | [44,45] |
| | uracil | Au(111) | Assembly | Co-assembly (chiral separation) + catassembly (structural transformation) | [26] |
| | cytosine | Au(111) | Assembly | Catassembly (structural transformation) | [47] |
| | guanine | Au(111) | Reaction | Tautomerization | [46] |
| CO | Co/Fe-tetraphenylporphyrin; Fe-tetramethyl-tetraazaannulene | Ag(111) | Assembly | Co-assembly (axial ligation, influencing the geometrical and electronic structures) | [53,55] |
| | Sierpiński triangles (Fe atoms and 4,4′′-dicyano-1,1′:3′,1′′-terphenyl) | Au(111) | Assembly | Co-assembly (axial ligation, structural transformation) | [27] |
| $CO_2$ | Sierpiński triangles (Fe atoms and 4,4′′-dicyano-1,1′:3′,1′′-terphenyl) | Au(111) | Assembly | Catassembly (structural transformation) | [27] |
| | metal-organic chains (Au atoms and 1,4-phenylene diisocyanide units) | Au(111); Au(100) | Assembly | Co-assembly (lateral bonding, structural transformation) | [58,59] |
| $O_2$ | metal-organic coordination networks (Fe atoms and 1,4-benzenedicarboxylic acid); {5,10,15,20-tetraphenylporphyrinato}Mn(III)Cl; organometallic structures | Cu(001); Ag(111); Cu(111) | Assembly | Co-assembly (structural transformation, dissociation) | [50,51,69] |
| | 3,6-di-2-pyridyl-1,2,4,5-tetrazine and Ag/Fe atoms | Ag(111) | Reaction | Self-metalation, metal replacement | [68] |
| | 1,3,5-tris(4-ethynylphenyl)benzene; poly(para-phenylene); 4,4′-diethynyl-1,1′-biphenyl; 4′-ethynyl-[1,1′-biphenyl]−4-ol; 4,4′-diethynyl-2,2′-bipyridine | Ag(111); Cu(111); Au(111); Ag(100) | Reaction | C–H activation | [28,29,70,71,73] |
| $H_2$ (molecular and atomic hydrogen) | manganese phthalocyanine; (3,1)-chGNRs, ketone-GNRs | Au(111) | Reaction | Hydrogenation | [48,74] |
| | Br by-products | Au(111); Cu(111); Cu(110) | Reaction | Removal of halogen residues | [60,62,63,65] |
| | tribromo-substituted dimethylmethylene-bridged triphenylamine; surface organometallics; 10,10′-dibromo-9,9′-bianthryl | Ag(111); Au(111), | Reaction | H passivation, debromination | [61–63] |
| | S-doped 5-AGNRs | Au(111) | Reaction | Desulfurization | [62] |
| | polycyclic aromatic hydrocarbons | Au(111) | Reaction | Superhydrogenation and covalent coupling | [64] |

of uracil (U) molecules on Au(111) via co-assembly.[26] Such a process is accompanied by the variation of the surface organic nanostructures from the racemic disordered U self-assembled structure (Figure 3b) to the homochiral ordered U+$H_2O$ structure (Figure 3c) at room temperature (RT). Submolecularly resolved STM images (Figure 3d–f,h) clearly show that homochiral U+$H_2O$ structures with different chiralities are composed of alternating five-membered U rings with single $H_2O$ molecules located at the center (appearing as dim dots as depicted by white circles). Bond-resolved nc-AFM images (Figure 3g,i) further resolved the intermolecular hydrogen bonds between $H_2O$ and U molecules. Interestingly, after keeping the U+$H_2O$ sample at RT for 90 min, a racemic ordered U self-assembled structure was obtained with the desorption of $H_2O$ molecules, which was also available by directly annealing the racemic disordered U structure at 330 K. It thus indicates the "catassembler" role of $H_2O$ molecules and the homochiral ordered U+$H_2O$ structure as an intermediate phase in the catassembly. Notably, such chiral separation is theoretically attributed to the preferential hydrogen-bonding interaction between water and U molecules at specific sites, with the formation of homochiral $(U-H_2O-U)_2$ cluster for subsequent chiral amplification. Therefore, such a water-driven co-assembly and catassembly process unambiguously displays the influence of $H_2O$ molecules on the structural transformation


© 2025 Wiley-VCH GmbH

23669608, 0, Downloaded from https://onlinelibrary.wiley.com/doi/10.1002/smtd.202402118 by Tongji University, Wiley Online Library on [07/04/2025]. See the Terms and Conditions (https://onlinelibrary.wiley.com/terms-and-conditions) on Wiley Online Library for rules of use; OA articles are governed by the applicable Creative Commons License

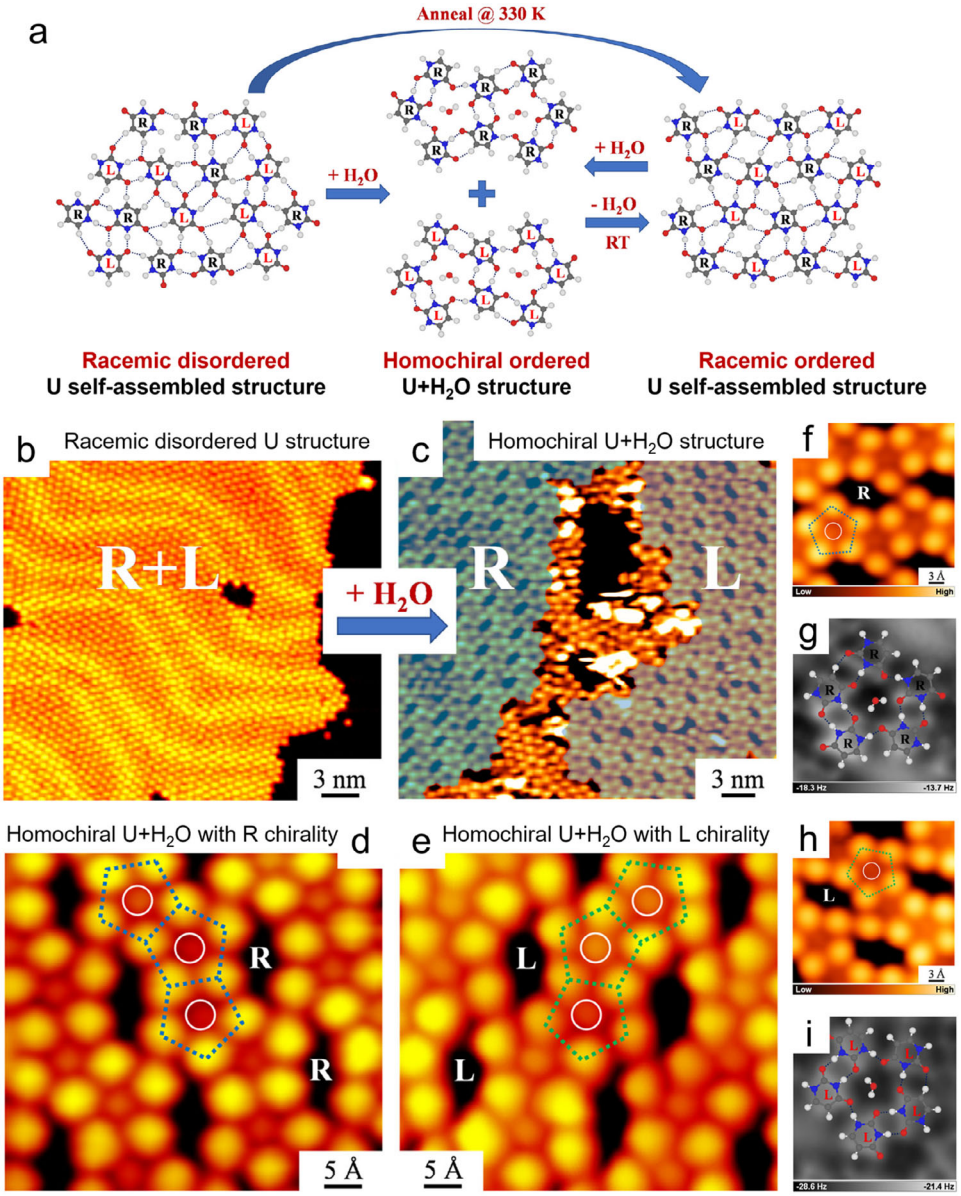


**Figure 3.** $H_2O$-mediated co-assembly and catassembly of U nanostructures. a–i) $H_2O$-induced chiral separation of racemic disordered U self-assembled structures on Au(111) to form homochiral U+$H_2O$ nanostructures with $H_2O$ molecules embedded at the center of U pentamers, followed by the formation of a racemic ordered U self-assembled structure. Reproduced with permission.[26] Copyright 2021, American Chemical Society.

of surface organic nanostructures, indicating their vital role in the biologically related systems.

In addition to the global hydration processes described above, the $H_2O$-mediated construction and modification of organic nanostructures can also be reversely interpreted by directly manipulating the $H_2O$ molecules involved (that is, local dehydration), as typically illustrated in **Figure** 4a. Thymine (T) molecules[45] were applied and hydrated to form a well-ordered water-involved T structure as a model system (Figure 4b), which consists of four hydrogen-bonded T dimers (depicted by green and blue contours) with different chiralities (R and L), surrounding a central $H_2O$ molecule (shown as a bright protrusion). It is worth noting that the two adjacent green T dimers interact with the $H_2O$ molecule via OH···O hydrogen bonds (Figure 4a), stabilizing the hydrated structure. The T+$H_2O$ nanostructure can withstand thermal treatment up to ≈350 K without breaking the arrangement before desorption, which is relatively strong and different from the situations of cytosine[47] and uracil.[26] Accordingly, such a system was applied to directly capture the influence of $H_2O$ molecules on the local intermolecular interactions in real space. After removal of the $H_2O$ molecules on both sides of the target green T dimer, the T dimer underwent a local chiral inversion process while preserving its hydrogen-bonding configuration (Figure 4d,e). Interestingly, when only a


© 2025 Wiley-VCH GmbH

23669608, 0, Downloaded from https://onlinelibrary.wiley.com/doi/10.1002/smtd.202402118 by Tongji University, Wiley Online Library on [07/04/2025]. See the Terms and Conditions (https://onlinelibrary.wiley.com/terms-and-conditions) on Wiley Online Library for rules of use; OA articles are governed by the applicable Creative Commons License

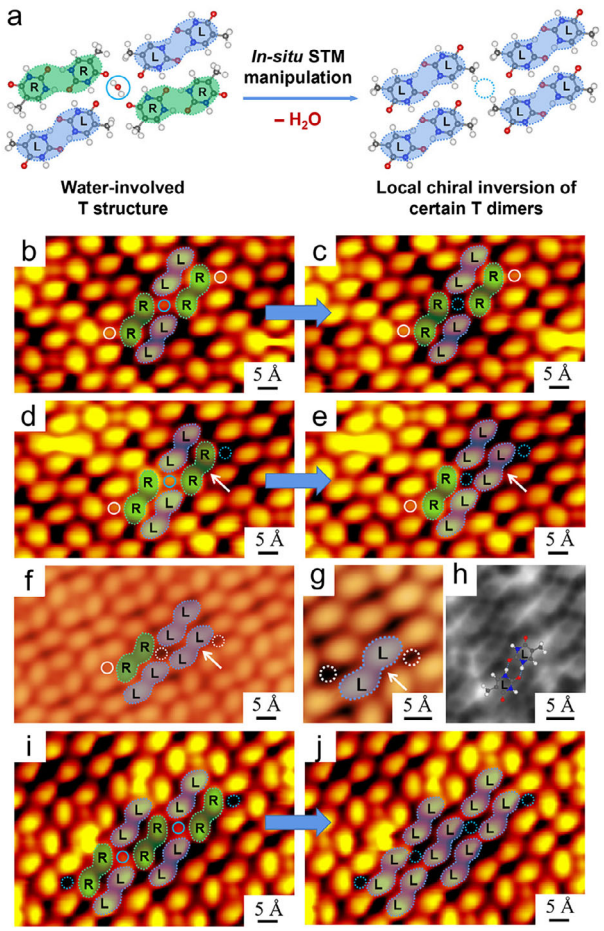


**Figure 4.** $H_2O$-mediated co-assembly of T nanostructures. a–j) Local chiral inversion of T dimers involved in the hydrated T+$H_2O$ nanostructures on Au(111) induced by STM manipulations on individual $H_2O$ molecules, showing a local dehydration process. Reproduced with permission.[45] Copyright 2022, American Chemical Society.

single $H_2O$ molecule was removed from one side, the green T dimer remained unchanged (Figure 4b,c). Significantly, when the $H_2O$ molecules on both sides of three T dimers were completely removed, all three T dimers experienced local chiral inversions (Figure 4i,j). The attribution of the chiral inversion was also examined by the bond-resolved nc-AFM image (Figure 4h) of the hydrated structure with naturally existing water vacancies (Figure 4f,g). Thus, by means of the tip-induced local dehydration, the interactions between water and organic molecules were directly identified and detected in real space. It thus paves the way for the fundamental understanding of water-driven assembly processes of organic molecules.

For more exhaustive examples involving water molecules, readers are suggested to refer to our recent review paper[20] on the interactions between extrinsic water molecules and organic molecules as well as inorganic salts (including ions) on surfaces. It describes first steps of hydration and microsolvation, tautomerization, chiral separation, structural transformation, and dissolution of salts and hydration of ions with the involvement of water molecules.

### 2.2. CO and $CO_2$

In addition, gas molecules such as $H_2$,[48] $NH_3$,[49] $O_2$,[50,51] NO,[52–54] and CO[53,55] are also commonly applied in the surface molecular systems. It has been reported that they allow the modification of the single-molecule morphology and/or assembled structures and, more importantly, the modulation of the electronic properties of metal-centered molecules (e.g., metal phthalocyanines/porphyrins) by their longitudinal adsorption. For example, the coordination of NO and oxygen to the metal centers modified the electronic interactions between the metal centers and the underlying surfaces,[56] as well as the oxidation states of metals[51,57] (e.g., the surface *trans* effect based on the weakening of the molecule-surface interactions upon gas coordination[57]). Moreover, Ballav et al. discovered that NO adsorption on cobalt(II)-tetraphenylporphyrin (CoTPP) coupled to Ni(001) and thermal dissociation can reversibly modulate the spin state transition of Co (that is, "off" and "on" states of the Co spin, respectively),[54] based on the combination of X-ray magnetic circular dichroism spectroscopy, XPS measurement, and STM observations. Such a study reveals the intriguing role of NO (or other gas molecules in certain molecule-substrate systems in general) as a chemical switch that efficiently controls the on/off switching of surface-adsorbed molecular spins.

In this context, we take the case of axial CO bonding on a Fe-tetramethyl-tetraazaannulene (FeTMTAA) molecule adsorbed on Au(111) reported by Berndt et al. as an example (**Figure 5**).[55] The CO ligation enabled the lateral bonding among molecules and thus modified the molecular assembly and the electronic properties, presenting a surface *cis* effect. At low coverages (e.g., 0.2 ML as shown in Figure 5a), in the absence of CO molecules, pristine FeTMTAA molecules were discretely distributed on Au(111), appearing as elongated hexagons. Upon exposure to CO molecules at a condition of $\approx 4 \times 10^{-5}$ mbar for 30–40 min, these CO-FeTMTAA molecules aggregate to form ordered trimers and chains with a drastic rearrangement (Figure 5b), indicating the influence of the CO ligand on the intermolecular interactions. Besides, a depression was found at the center of single molecules, exhibiting the variation in the single-molecule morphology as well. Such an influence was also valid at a higher coverage (≈0.5 ML), where double rows of FeTMTAA transformed to zigzag chains consisting of CO-FeTMTAA trimers upon addition of CO as shown in Figure 5c–f, respectively. Moreover, the CO-induced modification on the electronic properties was demonstrated by both STS spectra and DFT calculations (Figure 5g–i). The adsorption of CO onto FeTMTAA reduced the charge transfer between the molecular complex and the Au(111) surface by charge redistribution, leading to the largely neutral state of CO-FeTMTAA. The resulting CO-FeTMTAA exhibited electronic features similar to those of adsorbed NiTMTAA rather than those of pristine FeTMTAA from the dI/dV spectra (Figure 5i). Therefore, the vertical coordination by CO changes the molecular geometric structure, weakens the molecule-substrate interactions, and affects the lateral electrostatic interaction among FeTMTAA molecules, which is eventually reflected in the distinct molecular arrangements.

Apart from the modification of metal centers in single molecules, gas molecules can also assist structural transitions at the sub-monolayer level by axial coordination to the metal nodes


© 2025 Wiley-VCH GmbH

23669608, 0, Downloaded from https://onlinelibrary.wiley.com/doi/10.1002/smtd.202402118 by Tongji University, Wiley Online Library on [07/04/2025]. See the Terms and Conditions (https://onlinelibrary.wiley.com/terms-and-conditions) on Wiley Online Library for rules of use; OA articles are governed by the applicable Creative Commons License

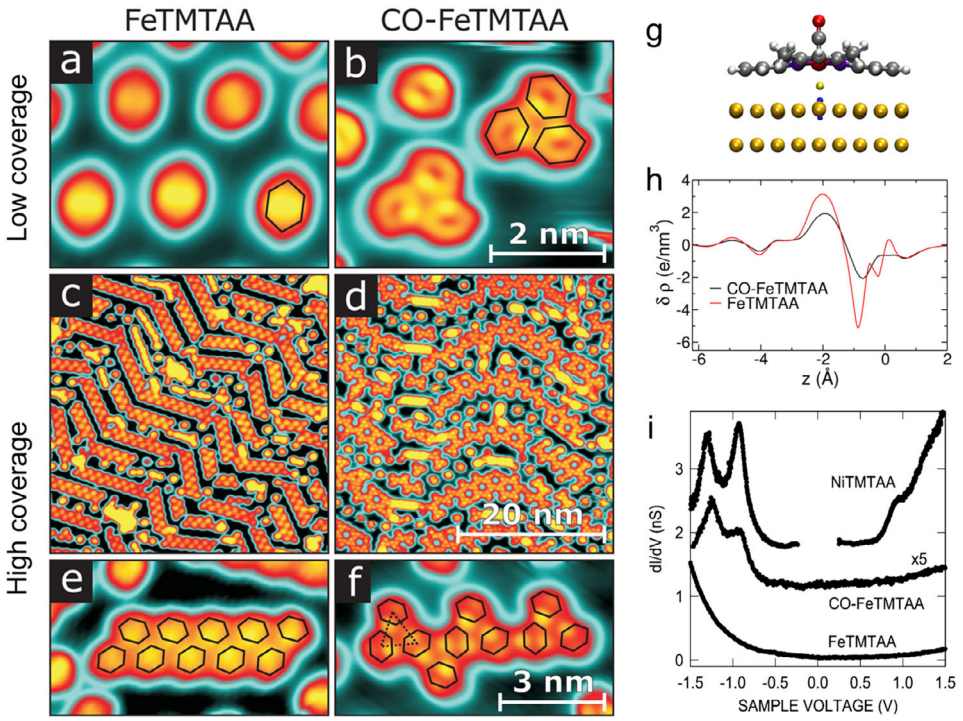


**Figure 5.** CO-induced axial bonding to FeTMTAA molecules, forming CO-FeTMTAA and lateral bonding among the molecules. a–f) Rearrangement of molecular assembled structures induced by the addition of CO molecules on Au(111) at different coverages. g–i) Induced density and charge in the CO-FeTMTAA complex and variation in the electronic properties. Reproduced with permission.[55] Copyright 2016, American Chemical Society.

involved in extended metal-organic nanostructures, while different species of gas molecules exhibit distinct behaviors in such processes. Remarkably, Wang et al. clearly visualized the different effects of CO and $CO_2$ on a special molecule-metal coordination structure, Sierpiński triangles (STs) assembled from Fe atoms and 4,4′′-dicyano-1,1′:3′,1′′-terphenyl (C3PC) molecules on Au(111),[27] as shown in **Figure 6**. After co-deposition of C3PC molecules and Fe atoms and subsequent annealing, subtle STs (i.e., $Fe(C3PC)_3$) were constructed with 3-fold coordination of Fe involved, where Fe atoms were not apparently visible at the center (Figure 6a,b). By dosing CO molecules at a pressure of $5.0 \times 10^{-6}$ Torr for 2 min (i.e., 600 L) to such a sample held at RT, obvious structural transformation was triggered. Regular long chains consisting of $FeCO(C3PC)_4$ via the 4-fold Fe···N coordination bonding appeared (Figure 6c,d). Interestingly, axially bonded CO molecules (indicated by white arrows in Figure 6c) to Fe atoms caused the protrusions at these positions, which could be desorbed from Fe by locally applying a voltage pulse of 2 V. In addition, CO exposure ($1.0 \times 10^{-8}$ for 100 s, i.e., 1 L) at a low temperature (≈30 K) resulted in the attachment to Fe centers in STs, forming $Fe_x(CO)_y$ clusters. A reverted transition from 1D chains to STs was further induced by annealing the sample with the desorption of CO. Thus, the introduction of CO molecules to STs resulted in the co-assembly of these species.

On the contrary, when $CO_2$ molecules were dosed at a pressure of $5.0 \times 10^{-6}$ Torr for 130 s (650 L) on a ST sample at RT, similar long chains were also formed, but with much fewer protrusions at Fe centers (Figure 6e,f). Low-temperature (≈30 K) dosing of $CO_2$ started to induce an obvious structural change only until it reached 60 L (Figure 6g), different from the situation of CO (1 L). Some typical $CO_2$-involved clusters, $Fe_x(CO_2)_y$, were displayed in Figure 6h–k. Accordingly, in the case of $CO_2$, a molecular catassembly process was demonstrated instead. The authors also rationalized the difference between CO and $CO_2$ from the standpoint of theoretical calculations, as CO prefers to coordinate with Fe centers, which is thermodynamically induced, while a high dosage of $CO_2$ plays a vital role in this gas-mediated structural transition.

Moreover, in some other cases, e.g., studies by Petek et al.,[58,59] the introduction of $CO_2$ molecules (at 90 K) induced the attractive interchain interactions via co-assembly. It thus resulted in surface structural changes with dispersed metal-organic chains gathering into close-packed bundles on Au(111), where $CO_2$ was laterally trapped (instead of vertically in the above reports) and $CO_2$-Au interactions played an important role.

Overall, these surface science studies demonstrate the dual modulation capability of gas molecules on i) the arrangements of pre-adsorbed molecular structures, and ii) the properties of individual molecules. This is possible because gas molecules affect the surface adsorbed molecules themselves and the intermolecular forces (or more generally, the interactions among all the components involved) in the molecular structures.

### 2.3. $O_2$ and $H_2$

In contrast to the less reactive gas molecules discussed above, some reactive gas molecules can usually act as reactants, not only


© 2025 Wiley-VCH GmbH

23669608, 0, Downloaded from https://onlinelibrary.wiley.com/doi/10.1002/smtd.202402118 by Tongji University, Wiley Online Library on [07/04/2025]. See the Terms and Conditions (https://onlinelibrary.wiley.com/terms-and-conditions) on Wiley Online Library for rules of use; OA articles are governed by the applicable Creative Commons License

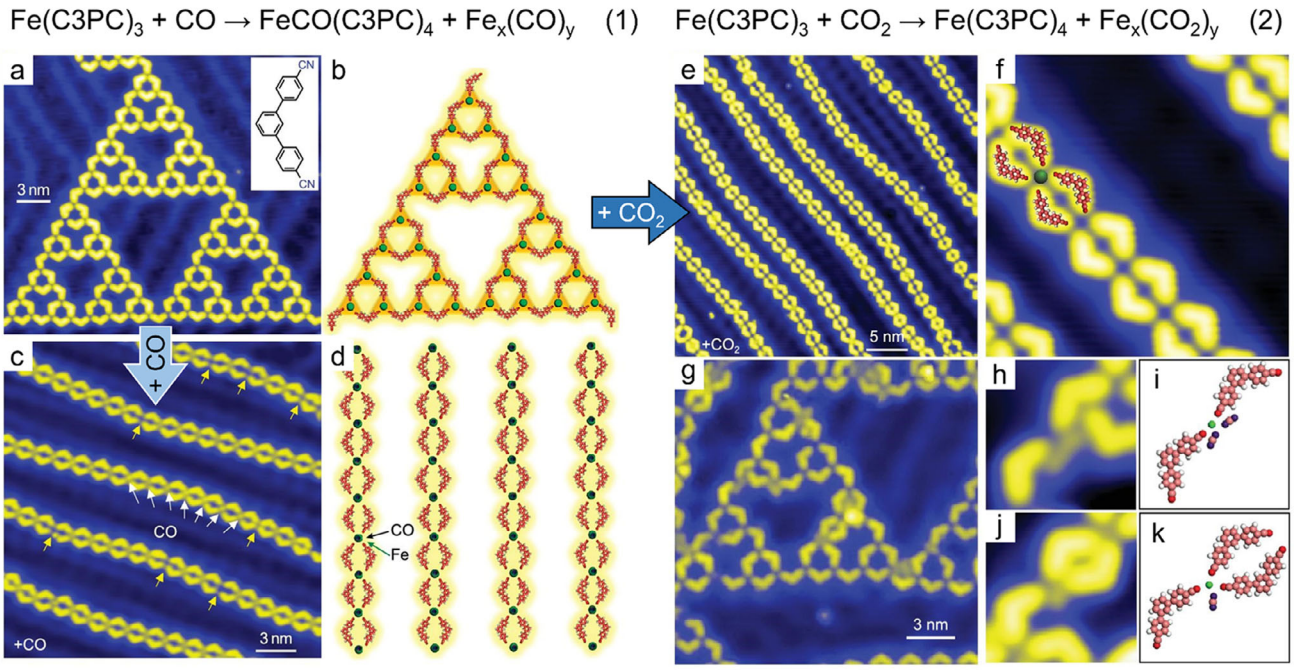


**Figure 6.** CO- and $CO_2$-assisted phase transitions from Sierpiński triangles to 1D chains via co-assembly and catassembly, respectively. a–d) Structural transformation from STs to 1D chains on Au(111) induced by CO molecules, which are axially bonded to Fe atoms. e,f) Formation of 1D chains on Au(111) induced by $CO_2$ molecules, which are absent in the chain structures. g–k) Intermediate structures with the coexistence of $CO_2$ and STs obtained after low-temperature (≈30 K) dosing of $CO_2$. Reproduced with permission.[27] Copyright 2023, Oxford University Press.

to assist in the reduction of reaction by-products, but also to react with molecular structures or catalyze reactions on surfaces. For instance, it has been widely established in diverse molecular systems that the introduction of $H_2$ into on-surface dehalogenative coupling reactions is a versatile strategy for the removal of halogen by-products.[60–65] Besides, Godlewski and co-workers have successfully realized many reaction processes based on atomic hydrogen by cracking $H_2$,[62] such as effective removal of halogen residues from Ullmann-type reactions, induced H-passivation of organometallic (OM) intermediate states, and debromination and desulfurization of adsorbed species on a Au(111) surface.

In addition to the reductive gas $H_2$, $O_2$, as the dominant reagent in oxidative chemistry,[34] plays an equally pivotal role in surface chemical reactions.[32,50,66,67] It has been reported by Tait et al. that $O_2$ can facilitate the self-metalation and metal replacement reaction processes of organic molecules by reducing the reaction temperatures.[68] Besides, Klappenberger and co-workers showed that $O_2$ served as an effective agent to induce the surface reaction of terminal alkynes, leading to the formation of 2D OM alkynyl–silver networks on Ag(111) at a micrometer scale. Interestingly, no $O_2$ residues or related by-products were found on the surface. This displays an excellent gas-mediated synthetic protocol and will be discussed in detail in **Figure 7**a,b.[28] Chi et al. also reported that $O_2$ induced further reactions of surface OM intermediate structures,[69] and acted as a catalyst in the lateral dehydrogenative fusion of polyphenylene chains to produce GNRs by drastically reducing the reaction temperature on Cu(111).[70]

Therefore, both reductive (e.g., $H_2$) and oxidative (e.g., $O_2$) gas molecules can be applied to promote specific surface chemical reaction processes and corresponding structural constructions, while some of the gases end up being completely desorbed without forming residual by-products. In this section, the surface organic nanostructures mediated by the introduction of such typical gas molecules, $O_2$ and $H_2$, and the corresponding reaction processes will be mainly discussed.

Figure 7 shows two typical examples of oxygen-catalyzed C–H activation of terminal alkynes on metal surfaces. In the work of Klappenberger et al., a molecular precursor of 1,3,5-tris(4-ethynylphenyl)benzene (Ext-TEB, see Figure 7a) was applied and deposited on Ag(111). Dosing $O_2$ (≈6000 L) onto an Ext-TEB-precovered Ag(111) sample held at 200 K efficiently resulted in the deprotonation of terminal alkynyl groups, while adsorbed oxygen or oxygen-containing species were absent from the sample, as evidenced by both STM observations and XPS measurements. Subsequent annealing at 375 K led to the construction of highly regular alkynyl–silver networks at a micrometer scale via the incorporation of thermally released Ag adatoms, which was confirmed by the STM topography, low-energy electron diffraction (LEED) pattern, and DFT model as shown in Figure 7b.

Thereafter, based on the similar strategy, by introducing $O_2$ into another molecular system of 4,4′-diethynyl-1,1′-biphenyl (DEBP) on Ag(111),[71] Kim and co-workers demonstrated that the on-surface reaction pathways of terminal alkynes could be successfully steered from C–C coupling[72] to C–H activation[71] with high selectivity at different statuses (Figure 7c). Notably, without the participation of $O_2$, thermal treatment of DEBP-preassembled Ag(111) sample led to the non-dehydrogenative direct addition reaction of terminal alkynyl groups, forming 1D long chains with predominantly C–C coupled enzyme connections. In contrast, upon the controllable addition of $O_2$ (≈200 L)


© 2025 Wiley-VCH GmbH

23669608, 0, Downloaded from https://onlinelibrary.wiley.com/doi/10.1002/smtd.202402118 by Tongji University, Wiley Online Library on [07/04/2025]. See the Terms and Conditions (https://onlinelibrary.wiley.com/terms-and-conditions) on Wiley Online Library for rules of use; OA articles are governed by the applicable Creative Commons License

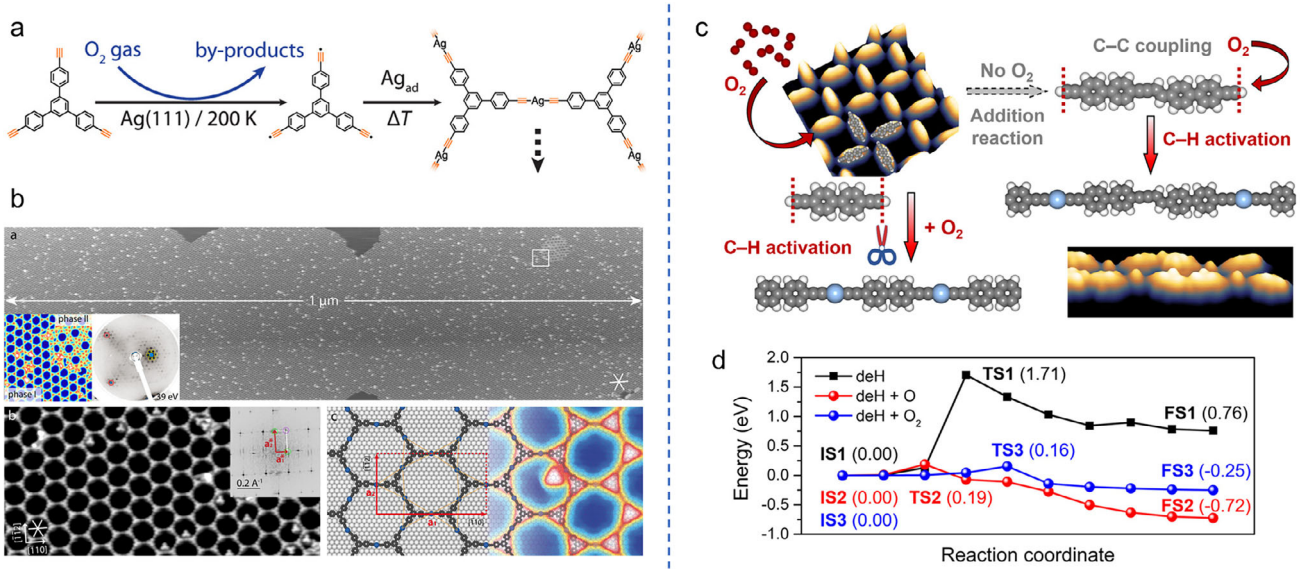


**Figure 7.** $O_2$-facilitated C–H activation reactions of terminal alkynes forming OM nanostructures on surfaces. a,b) $O_2$-mediated construction of 2D regular alkynyl–Ag– alkynyl OM networks on Ag(111) at the micrometer scale. Reproduced with permission.[28] Copyright 2019, American Chemical Society. c,d) Oxygen-facilitated regulation of reaction pathways of terminal alkynes from C–C coupling to C–H activation on Ag(111). Reproduced with permission.[71] Copyright 2022, American Chemical Society.

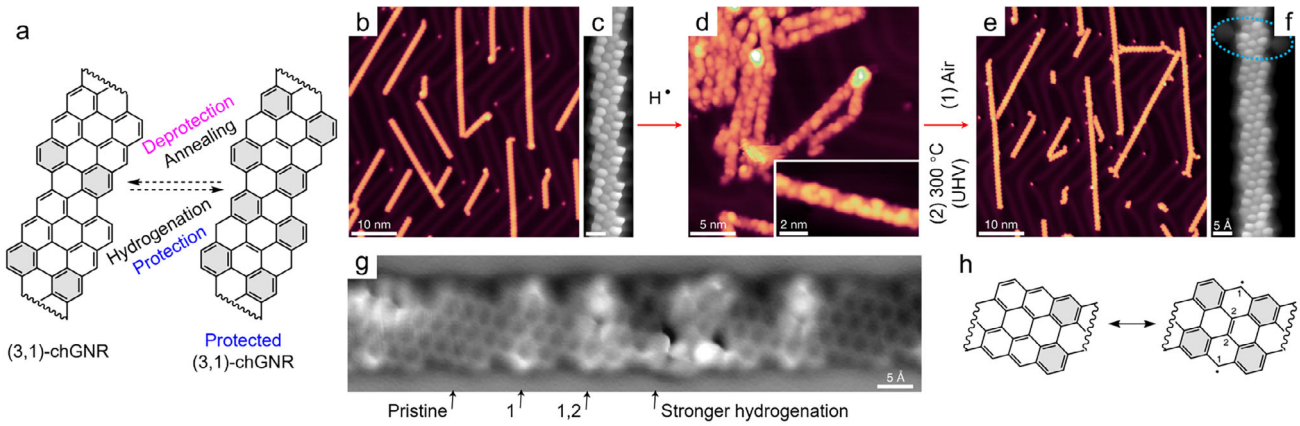


**Figure 8.** Hydrogen-induced protection of (3,1)-chGNRs that survive exposure to air. a) Schematic illustration of the protection and deprotection of GNRs on Au(111). b–g) Synthesis, hydrogenation protection, and deprotection of (3,1)-chGNRs. h) Two resonant forms of a chGNR unit cell. Reproduced with permission.[74] Copyright 2022, Springer Nature.

to the DEBP-precovered Ag(111) sample held at RT, the C–H activation process was facilitated, along with the formation of long extended 1D OM chains that gathered into close-packed islands. Furthermore, the active oxygen species (both molecular and atomic oxygen) were selectively introduced and induced H abstraction via an associative or dissociative mechanism, respectively. DFT calculations further verified that the involvement of either oxygen species could induce a drastic reduction in the reaction barrier of C–H activation (from 1.71 eV to less than 0.2 eV) via hydrogen bonding with terminal alkynyl groups. Consequently, the introduction of $O_2$ allows the C–H activation to occur (at lower than RT) rather than C–C coupling, as well as the selective regulation of reaction pathways. Moreover, such a strategy is also applicable on Au(111), but in a less efficient way.

Recently, as an extension of the above systems of terminal alkynes, Yang and co-workers further modified the molecular precursor by adding a directing hydroxyl group and realized the highly selective synthesis of enediynes on Ag(100) induced by $O_2$ exposure.[73]

These above studies demonstrate the great potential of gas molecules in assisting the mesoscopic synthesis of various surface nanostructures, ranging from 2D nanoporous networks, 1D nanochains, to 0D single molecules.

In the case of $H_2$, in addition to its versatile application in the removal of halogen by-products,[60–65] it has also been subtly applied to protect GNRs with zigzag edges on Au(111) by de Oteyza and co-workers (**Figure 8**).[74] To circumvent the stability problems of GNRs,[75] well-ordered (3,1)-chGNRs prepared


© 2025 Wiley-VCH GmbH

23669608, 0, Downloaded from https://onlinelibrary.wiley.com/doi/10.1002/smtd.202402118 by Tongji University, Wiley Online Library on [07/04/2025]. See the Terms and Conditions (https://onlinelibrary.wiley.com/terms-and-conditions) on Wiley Online Library for rules of use; OA articles are governed by the applicable Creative Commons License

**Table 2.** Summary of the application of some typical extrinsic metals in the preparation of surface organic nanostructures by reactions.

| Category of Extrinsic metals | Metals | Target organic molecules | Substrates | Roles | Refs. |
|---|---|---|---|---|---|
| Transition metals | Cu atoms | Br-substituted porphyrins; 5,15-bis-(4-bromophenyl)-10,20-diphenyl porphyrin | Au(111) | Catalyzing Ullmann coupling (+ template effect) | [86,87] |
| | Pd atoms | 5,15-bis-(4-bromophenyl)-10,20-diphenyl porphyrin | Au(111) | Catalyzing Ullmann coupling | [87] |
| | Ni atoms | 10,10′-dibromo-9,9′-bianthryl | Au(111) | Catalyzing debromination and fusion reaction | [88] |
| | Fe atoms | 1,4-bis(6,6″-dibromo-[2,2′:6′,2″-terpyridin]-4′-yl)benzene; 4,4′-(1,4-phenylene)dipyridine | Au(111) | Guiding the reaction pathway (+ template effect); catalyzing selective C−H activation (+ template effect) | [89,95] |
| | Au atoms | 9,10-dicyanoanthracene | Ag(111) | Catalyzing aromatic C−H activation | [93] |
| Lanthanide metals | Dy atoms | 4,4″-dibromo-p-terphenyl | Ag(111) | Catalyzing dehalogenation but inhibiting Ullmann coupling reaction | [90] |
| Alkali metals | Na atoms | 4,4′-dibromo-2,2′-diiodo-1,1′-biphenyl, 4,4″-dibromo-1,1′:4′,1″-terphenyl; 4,4′-dibromo-2,2′-bipyridine; 4,4′-diethynyl-2,2′-bipyridine | Au(111); Ag(111) | Catalyzing dehalogenation, isolating halogen residues; controlling the selectivity of reaction products; directing the organometallic nanostructures | [30,91,29] |
| | NaCl | guanine | Au(111) | Facilitating the tautomerization | [31] |
| | NaCl (+ Ag atoms) | hexaazatriphenylene | Ag(111) | Catalyzing selective C−H activation and polymerization | [94] |

on Au(111) (Figure 8b,c) were intentionally exposed to atomic hydrogen (by cracking $H_2$), leading to the formation of hydrogenated ribbons with drastic changes in the contrast in STM images (Figure 8d). A representative nc-AFM image of lightly hydrogenated ribbons clearly displays the morphologic difference and the presence of pristine unit cells (Figure 8g). The reactivity of these ribbons was attributed to a minor contribution of an open-shell resonant form (Figure 8h). Such hydrogenated protected GNRs were then exposed to the ambient atmosphere, and the sample was transferred back to the UHV chamber followed by annealing at 300 °C to remove co-adsorbed contaminants and to further deprotect (i.e., dehydrogenate) the GNRs. Amazingly, ≈90% of the chGNR units were found to be pristine (Figure 8e,f) with retained electronic properties, exhibiting the vital role of hydrogen in protecting pristine GNRs from the oxidizing effects of the atmosphere. Moreover, hydrogen (in the atomic form) exposure followed by annealing at 330 °C also successfully deprotected ketone-GNRs (i.e., the pre-oxidized form functionalized with ketone side groups), which reconverted to mostly pristine forms. Thus, both strategies demonstrate the great potential of hydrogen in regulating the reaction processes and protecting nanostructures and their electronic properties, which can hopefully be extended to other systems of carbon-based nanostructures and bridge the gap between UHV experimental conditions and real-world application scenarios.

## 3. Extrinsic Metals

In this section, several typical examples of surface organic nanostructures mediated by various extrinsic metal elements, ranging from transition metals to alkali metals, will be briefly reviewed. Due to the availability of a large number of excellent reviews[6,21,22,76–78] on the assembly of metal atoms and organic molecules on surfaces, we will skip relevant parts and focus mainly on some chemical reactions (C−X and C−H activation) and corresponding organic nanostructures mediated by extrinsic metals (also see **Table 2**).

The well-known Ullmann-type dehalogenative coupling reactions have been extensively applied in the synthesis of extended functional nanostructures based on the pre-designed halogen substitutions and sites.[8,9,79–81] Whereas, they suffer from several practical problems, such as surrounding halogen by-products and high C–X (X: halogen) activation temperatures, which greatly hinder the extension of nanostructures and further property characterization. These incompatible features make dehalogenative reactions intriguing molecular systems to explore and to regulate on surfaces. They have attracted contributions from molecular design,[82–84] halogens-to-halides (e.g., HBr) conversion facilitated by extrinsic $H_2$[60–65] (as discussed above), and Si-promoted conversion to $SiBr_4$ (followed by desorption).[85] On the other hand, the introduction of extrinsic metals into corresponding molecular systems has also proven to be an effective alternative strategy. For example, in the pioneering work of Lin and co-workers,[86] Cu atoms not only provided the metal-directed template effect, but also catalyzed the dehalogenative coupling reaction by lowering the reaction temperatures, facilitating the preparation of covalent organic nanostructures on Au(111). The catalytic performance of Cu atoms was further demonstrated in comparison with the application of Pd atoms. The rate-limiting steps in Cu- or Pd-catalyzed processes on Au(111) were revealed to be different (i.e., C–X activation and C–C coupling, respectively).[87] In addition, Ni atoms also acted as catalysts in facilitating debromination and further fusion of GNRs on Au(111).[88] Moreover, the incorporation of some other metal atoms, e.g., Fe, was shown to provide a metal-organic coordination template. Such a template is crucial for the selective synthesis of covalent coupling products with a specific molecular conformation on Au(111),[89] demonstrating the control over


© 2025 Wiley-VCH GmbH

23669608, 0, Downloaded from https://onlinelibrary.wiley.com/doi/10.1002/smtd.202402118 by Tongji University, Wiley Online Library on [07/04/2025]. See the Terms and Conditions (https://onlinelibrary.wiley.com/terms-and-conditions) on Wiley Online Library for rules of use; OA articles are governed by the applicable Creative Commons License

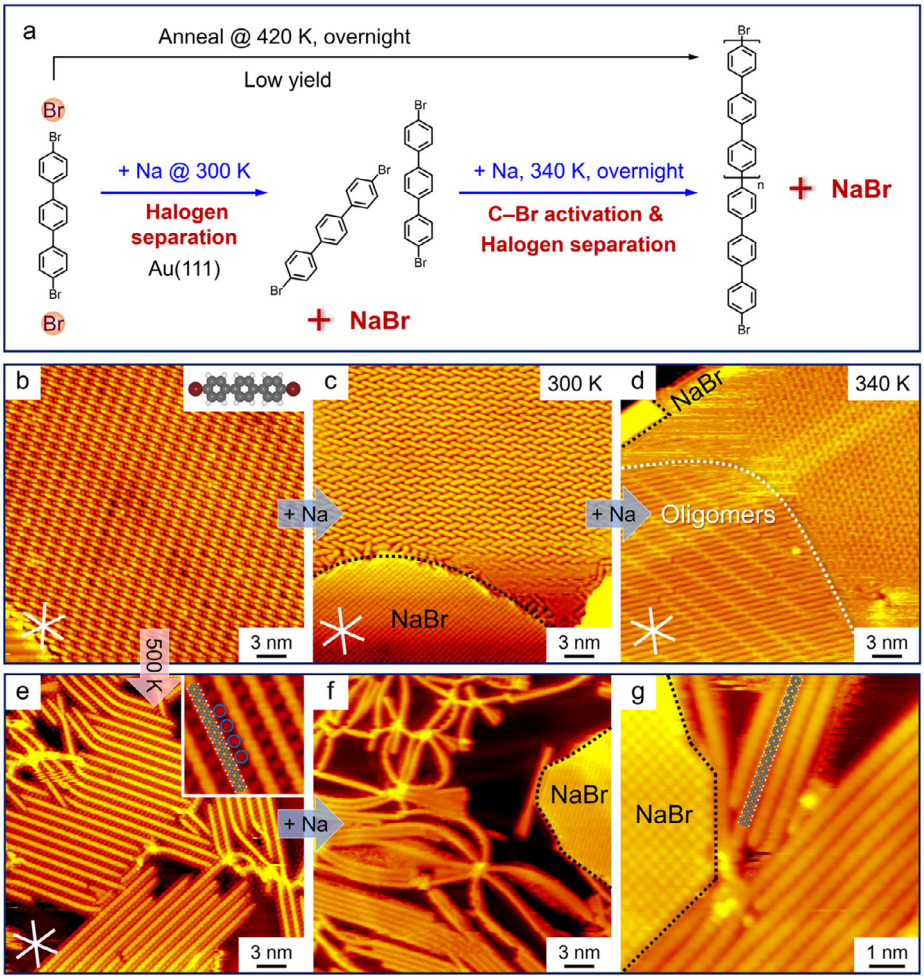


**Figure 9.** Na-facilitated halogen separation in the DBTP system on Au(111). a) Reaction processes of DBTP molecules in the presence and absence of Na. b–d) Structural transformations in response to the gradual addition of Na from b) mixed islands of DBTP and residual Br, through c) pure DBTP islands and separated NaBr islands, to d) appearance of islands of DBTP-based oligomers. e) Formation of long polyphenylene chains with dissociated Br atoms. f,g) Na-induced separation of polyphenylene chains and NaBr islands. Reproduced with permission.[30] Copyright 2024, American Chemical Society.

reaction pathways by extrinisic metals. Apart from these typical transition metals, lanthanide metals, such as Dy, have also been applied in the Ullmann coupling reactions on Ag(111),[90] which promoted the debromination with the formation of C–Dy–C OM structures, but unfortunately, inhibited further C–C coupling.

More recently, Xu and co-workers have demonstrated that the introduction of extrinsic alkali metal, Na atoms, into dehalogenative reactions on Au(111) is a versatile halogen separation strategy. It not only isolated the halogen by-products by forming NaX salt islands, but also assisted the C–Br activation under mild conditions (as shown in **Figure 9**).[30] The versatility of Na atoms was examined based on two molecular precursors functionalized with different halogen substitutions. The more general one, 4,4′′-dibromo-1,1′:4′,1′′-terphenyl (DBTP), will be taken as an example here (see Figure 9a). After dosing Na to the Au(111) sample of DBTP molecules mixed with residual Br atoms (Figure 9b) at 300 K, surrounding Br atoms were successfully separated from self-assembled pure DBTP islands, forming NaBr islands (Figure 9c). Further Na dosing followed by annealing at ≈340 K effectively triggered the C–Br activation with the appearance of DBTP-based oligomers (Figure 9d). In contrast, the reaction occurred with a low yield even after annealing at ≈420 K in the absence of Na (Figure 9a). Significantly, the Na-induced halogen separation strategy was also applicable to long 1D polyphenylene chains with dissociated interchain Br atoms obtained by annealing at ≈500 K (Figure 9e), which were also thoroughly separated away at RT (Figure 9f,g). Furthermore, DFT calculations revealed the Na-promoted reduction in the reaction barriers for C–Br activation and regulation of the reaction equilibrium by isolating halogens from the corresponding reaction systems. This Na-induced halogen separation strategy should be significant for the precise synthesis and property characterization of organic nanostructures, especially carbon-based nanostructures on surfaces.

As an extension, the influences of intrinsic Ag adatoms and extrinsic Na atoms were further compared in another dehalogenative reaction system on Ag(111).[91] It turned out that the addition


© 2025 Wiley-VCH GmbH

23669608, 0, Downloaded from https://onlinelibrary.wiley.com/doi/10.1002/smtd.202402118 by Tongji University, Wiley Online Library on [07/04/2025]. See the Terms and Conditions (https://onlinelibrary.wiley.com/terms-and-conditions) on Wiley Online Library for rules of use; OA articles are governed by the applicable Creative Commons License

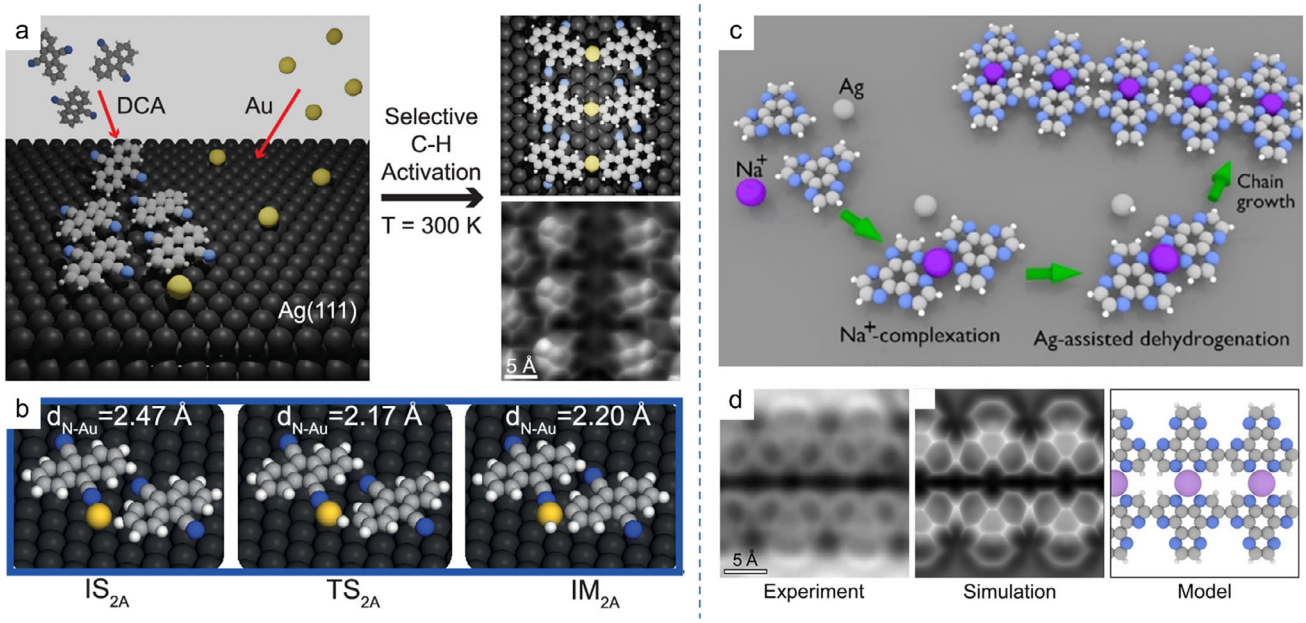


**Figure 10.** Extrinsic-metal-facilitated C–H activation on Ag(111). a,b) Au-catalyzed selective activation of aromatic C–H bonds of DCA molecules on Ag(111) at RT, forming OM DCA–Au–DCA dimers. Reproduced with permission.[93] Copyright 2022, American Chemical Society. c,d) Selective C–H activation facilitated by Na (from NaCl) and Ag adatoms on Ag(111), forming linear heteroaromatic polymers. Reproduced with permission.[94] Copyright 2021, John Wiley and Sons.

of Na atoms resulted in the control of the covalent coupling products with high selectivity, which were transformed from *trans*-chains (without the participation of Na) to isomerically specific *cis*-rings. It is also noteworthy that the connections and differences between alkali metal salts (e.g., NaCl) and pure alkali metal (e.g., Na) as extrinsic Na sources in the construction of metal-organic nanostructures and structural evolutions were also discussed recently.[92]

Moreover, extrinsic metals are also indispensable in some other on-surface reactions, typically like C–H activation. For instance, extrinsic Au atoms were co-deposited with 9,10-dicyanoanthracene (DCA) molecules onto Ag(111) and were found to catalyze the selective activation of aromatic C–H bonds at RT, along with the formation of C–Au–C OM structures (**Figure 10**a,b).[93] The structure, stability, and electronic properties of the DCA–Au–DCA dimer were characterized by STM imaging/manipulation, nc-AFM, and STS, respectively, providing atomic-scale experimental evidence for the single-Au-atom catalyzed regioselective C–H activation (Figure 10a). In addition, the reaction mechanism was further rationalized by DFT and quantum mechanics/molecular mechanics (QM/MM) calculations, where a Au–organic complex (via Au···N coordination) served as an intermediate to strongly reduce the dissociation barrier of the specific aromatic H (Figure 10b).

Selective C–H activation was also reported to be possible by the cooperative catalysis of Na (from NaCl) and Ag adatoms on Ag(111), which steered both the polymerization and the regioselectivity of the Scholl reaction (Figure 10c,d).[94] Co-deposition of hexaazatriphenylene (HAT) molecules and NaCl onto Ag(111) followed by annealing at 700 K resulted in the synthesis of linear heteroaromatic polymers (Figure 10c). The Na-involved double-chain structure of the polymers was determined by STM and nc-AFM characterization (Figure 10d). In contrast, annealing in the absence of NaCl resulted in the complete desorption of HAT molecules. DFT and QM/MM simulations suggested that the formation of $(HAT)_2$-Na complex (via Na···N interaction) increased the resistance against thermal treatment, while Ag adatoms catalyzed the C–H activation, thus cooperatively facilitating the polymerization reaction.

Similarly, Fe atoms provided 3-fold Fe···N coordination to target molecules with pyridine rings adsorbed on Au(111), which controlled the specific *ortho*-site C–H activation to selectively construct C–C coupling products.[95] Besides, Na from NaCl was shown to facilitate the tautomerization of a special biomolecule, guanine, on Au(111) via electrostatic intermolecular interactions.[31] These examples unexceptionally illustrate the significant roles that extrinsic metals have played in the molecular systems, not only in the bottom-up construction of nanostructures, but also in single-molecule reactions.

Therefore, the introduction of extrinsic metals (in the form of either pure metals or salts) into molecular reactions not only provides metal-organic template effects for the selective construction of covalent bonds, but also catalyzes reactions by lowering reaction temperatures or barriers. This should greatly broaden the regulatory strategies for on-surface synthesis and shed light on the preparation of well-defined covalent organic nanostructures for diverse applications in molecular electronics and nanodevices.

## 4. Cooperative Effects of Extrinsic Components

Finally, the combination of different types of extrinsic components (e.g., the integration of both small gas molecules and extrinsic metals) in the modification of surface organic


© 2025 Wiley-VCH GmbH

23669608, 0, Downloaded from https://onlinelibrary.wiley.com/doi/10.1002/smtd.202402118 by Tongji University, Wiley Online Library on [07/04/2025]. See the Terms and Conditions (https://onlinelibrary.wiley.com/terms-and-conditions) on Wiley Online Library for rules of use; OA articles are governed by the applicable Creative Commons License

nanostructures and their respective roles will be discussed using a recent example (**Figure 11**).

As mentioned in the $O_2$ section and in Figure 7, the introduction of extrinsic gas molecules, $O_2$, efficiently induces the C–H activation of terminal alkynes on Ag(111) at RT, leading to the construction of OM $C_{sp}$–Ag–$C_{sp}$ interlinked covalent nanostructures.[28,71] Due to both covalent and reversible features of C–M–C OM bonding, it is expected that distinct covalent OM polymers can be fabricated by tailoring internal factors or external stimuli.

In view of this, Xu and co-workers subtly regulated the intermolecular electrostatic interactions by introducing extrinsic Na atoms and organic molecules, PT (pyrene-4,5,9,10-tetraone), into the molecular system of terminal alkynes on Ag(111) (which was exposed to extrinsic $O_2$ gas to form 1D *trans* OM chains initially, see Figure 11a).[29] As a result, they successfully directed the ring–chain equilibrium of covalent OM nanostructures between *trans* OM chains and *cis* OM rings at RT under UHV conditions. The molecular precursor, 4,4′-diethynyl-2,2′-bipyridine (DEBPy), was employed, involving two terminal alkynyl groups for constructing C–Ag–C OM bonds and a bipyridyl moiety for interacting with extrinsic Na. Upon exposure to $O_2$ at RT, *trans* OM chains based on DEBPy molecules were synthesized on Ag(111) (Figure 11b). Intriguingly, the addition of Na to such a sample at RT efficiently led to the chain-to-ring conversion based on the *trans*-to-*cis* isomerization of DEBPy-based components and dynamic C–Ag–C covalent bonds, thus forming Kagome networks composed of *cis* OM rings and Na via 4-fold Na···N electrostatic interactions (Figure 11c–f). More interestingly, by further introducing PT molecules into the above system at RT, the preferential 4-fold Na···O (from PT) electrostatic interactions resulted in the removal of Na atoms from DEBPy-based molecular nanostructures, along with a reverse ring-to-chain conversion (Figure 11g–i).

Such a dynamic interconversion process was energetically driven, as demonstrated by DFT calculations on total energies of molecular systems with different binding sites of Na (Figure 11j). DFT-calculated reaction pathways for the *cis-trans* interconversion without and with the participation of Na further unraveled the mechanism for the dynamic ring–chain evolutions. The extrinsic Na lowered the reaction barrier of the *trans*-to-*cis* isomerization and, more importantly, converted the process from endothermic to exothermic, while PT-induced removal of Na allowed the reverse *cis*-to-*trans* isomerization. Such a study clearly demonstrates that the weak intermolecular interactions provided by extrinsic components can indeed govern the dynamics of covalent polymers at the submolecular level, which bridges the gap between supramolecular and covalent chemistry for the modification and control of surface organic nanostructures.

Therefore, the integration of different types of extrinsic components should be promising for providing cooperative effects, although there is relatively little research on this topic. On the one hand, due to the diverse chemical activities of gas molecules, they have unique advantages (e.g., high reversibility and controllability) in regulating the assembled structures, electronic properties, and reactions of target organic molecules adsorbed on surfaces. On the other hand, a wide range of extrinsic metals are available to provide additional metal-organic interactions (including template effects), direct molecular conformations, catalyze reactions, and steer reaction pathways on surfaces. Their combination will be an enrichment of the regulatory strategies for the preparation of surface organic nanostructures.

## 5. Conclusion

In conclusion, we have reviewed several typical case studies regarding the construction and modification of surface organic nanostructures mediated by extrinsic components through assembly and reaction, ranging from small gas molecules (predominantly including $H_2O$, CO and $CO_2$, $O_2$ and $H_2$) to metals, as well as their combinations. Taking advantage of extrinsic components with different chemical properties, surface organic nanostructures can be tailored in various aspects, including but not limited to assembled nanopatterns, formation and reaction processes, physicochemical properties, etc. Among others, more attention has been paid to the gas-mediated molecular assembly and reactions and the corresponding nanostructures and properties in this review, as they are the emerging topics of significance. In addition, the detailed roles that these extrinsic components play in the regulation of these assembly and reaction processes have been elucidated and summarized through both experimental and theoretical investigations.

Despite these attractive applications of extrinsic components in the preparation of surface organic nanostructures, several challenges still remain that require deeper experimental and theoretical understanding.

1) First, real-space and especially real-time visualization or detection of the extrinsic-components-mediated construction processes should be critical to the mechanistic studies for the further implementation of this strategy. In many of the cases discussed above, only the initial states (starting phases or structures) and final states (ending phases or structures) were observed with obvious structural transformations or reactions. The detailed processes and mechanisms mediated by extrinsic components were proposed mainly on the basis of theoretical calculations on simplified model systems instead. Such a situation may prohibit the correct and precise interpretation of these processes. It also hinders the understanding of the roles of extrinsic components and their interactions with the target organic molecules and nanostructures on surfaces. This is especially true for complicated processes such as catassembly and multicomponent reactions. In this sense, the advancement of *in-situ* spectroscopic techniques under various experimental conditions is expected to provide complementary experimental evidence other than topographic information, which should be essential to elucidate the regulatory mechanisms and to propose new theories of assembly and reactions induced by extrinsic components.
2) Second, the combination of extrinsic components (of the same or different types, for instance, the involvement of different types of metals[94] or the combination of extrinsic metals and gas molecules[29]) requires further exploration and is expected to play a distinct and unique role in influencing surface organic nanostructures. For example, ethylene epoxidation on silver catalysts, as one of the most significant oxidation reactions in the chemical industry, has been selectively promoted by the integration of typically Cs and Cl,[96]


© 2025 Wiley-VCH GmbH

23669608, 0, Downloaded from https://onlinelibrary.wiley.com/doi/10.1002/smtd.202402118 by Tongji University, Wiley Online Library on [07/04/2025]. See the Terms and Conditions (https://onlinelibrary.wiley.com/terms-and-conditions) on Wiley Online Library for rules of use; OA articles are governed by the applicable Creative Commons License

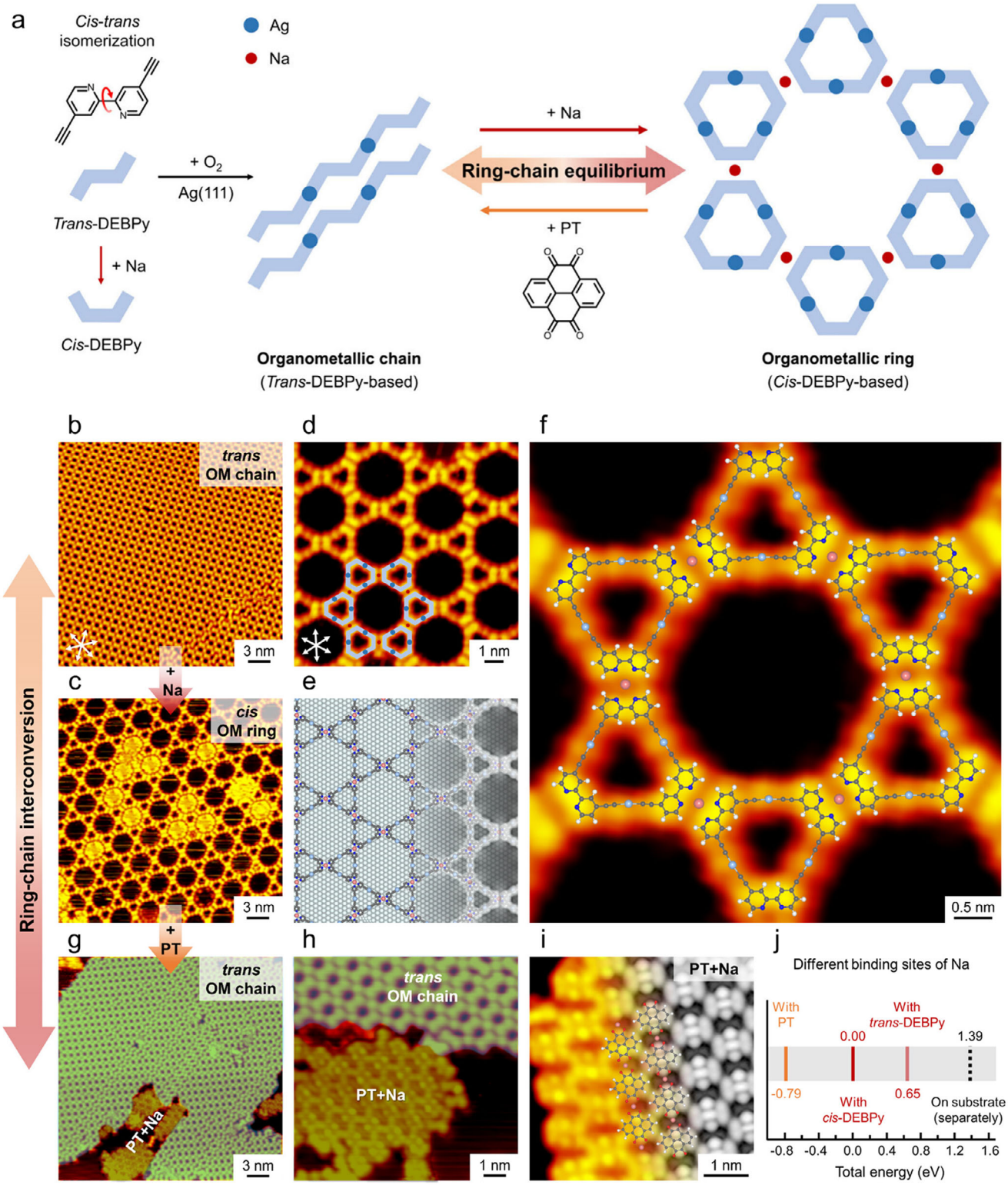


**Figure 11.** OM ring–chain equilibrium on Ag(111) determined by extrinsic components. a–i) Ring–chain interconversion between *trans* OM chains and *cis* OM rings in response to the addition of extrinsic Na atoms and PT molecules at RT, respectively. j) Total energies of molecular systems with different binding sites of Na. Reproduced with permission.[29] Copyright 2024, American Chemical Society.



© 2025 Wiley-VCH GmbH

23669608, 0, Downloaded from https://onlinelibrary.wiley.com/doi/10.1002/smtd.202402118 by Tongji University, Wiley Online Library on [07/04/2025]. See the Terms and Conditions (https://onlinelibrary.wiley.com/terms-and-conditions) on Wiley Online Library for rules of use; OA articles are governed by the applicable Creative Commons License

while the mechanistic understanding of such enhancement remains elusive. Atomic-scale investigation of such relevant model processes on surfaces should have practical implications for the optimization of catalytic performance for extensive applications. Currently, a limited number of studies have contributed to the combination of multiple extrinsic components, but have already demonstrated its promising prospect. Among others, the properties and characteristics of various individual extrinsic components in these processes should be the most fundamental part. On this basis, their combination will hopefully open up a new avenue for the preparation of surface organic nanostructures (e.g., cooperative catalysis) from our point of view.

3) Last but not least, the scope of extrinsic components should be further expanded and not be limited only to small gas molecules and metals. Recent studies have demonstrated that dehalogenated radicals derived from organic molecules other than the target ones can efficiently reduce the reaction temperatures of C–H activation of terminal alkynes on Ag(111), facilitating the formation of OM nanostructures.[97,98] These radicals would potentially expand the family of extrinsic components. Nevertheless, halogen residues and competitive processes of these radicals would be attendant problems. In this regard, some small and long-lasting radical molecules adsorbed on surfaces, capable of catalyzing specific on-surface reactions without participating in the reaction products, would be the extrinsic components of choice for the preparation of surface organic nanostructures. Thus, further in-depth exploration of potential extrinsic components and expansion of their family should be urgently pursued to increase the application versatility.

This new assembly and reaction methodology mediated by extrinsic components offers great opportunities to overcome some long-standing problems, such as harsh preparation conditions, poor selectivity, and side reactions, in the construction and modification of organic nanostructures and nanomaterials on surfaces. In addition, the underlying mechanisms elucidated in the surface model systems at the molecular scale are also valuable and inspiring for practical supramolecular engineering and nanomaterials development. This methodology is therefore expected to move surface chemistry a big step forward toward the precise and efficient construction and regulation of surface organic nanostructures and nanomaterials. They will have broad applications, including but not limited to the next-generation submicron-scaled molecular electronics and devices, catalysis, energy conversion, energy storage, etc.

## Acknowledgements

The authors acknowledge financial support from the National Natural Science Foundation of China (Grants Nos. 22202153 and 22125203) and the Fundamental Research Funds for the Central Universities. Chi Zhang was also grateful for the little baby in preparing the draft together during the late pregnancy and babyhood.

## Conflict of Interest

The authors declare no conflict of interest.

## Keywords

density functional theory, extrinsic components, molecular assembly, on-surface molecular reaction, scanning probe microscopy, surface organic nanostructures

Received: December 9, 2024
Revised: February 27, 2025
Published online:

[1] C. Joachim, J. K. Gimzewski, A. Aviram, *Nature* **2000**, *408*, 541.
[2] T. Harashima, Y. Hasegawa, S. Kaneko, M. Kiguchi, T. Ono, T. Nishino, *Angew. Chem., Int. Ed.* **2019**, *58*, 9109.
[3] W. B. Davis, W. A. Svec, M. A. Ratner, M. R. Wasielewski, *Nature* **1998**, *396*, 60.
[4] M. Irie, T. Fukaminato, K. Matsuda, S. Kobatake, *Chem. Rev.* **2014**, *114*, 12174.
[5] R. Otero, J. M. Gallego, A. L. V. de Parga, N. Martín, R. Miranda, *Adv. Mater.* **2011**, *23*, 5148.
[6] J. V. Barth, *Annu. Rev. Phys. Chem.* **2007**, *58*, 375.
[7] J. V. Barth, G. Costantini, K. Kern, *Nature* **2005**, *437*, 671.
[8] L. Grill, M. Dyer, L. Lafferentz, M. Persson, M. V. Peters, S. Hecht, *Nat. Nanotechnol.* **2007**, *2*, 687.
[9] L. Lafferentz, V. Eberhardt, C. Dri, C. Africh, G. Comelli, F. Esch, S. Hecht, L. Grill, *Nat. Chem.* **2012**, *4*, 215.
[10] L. Lafferentz, F. Ample, H. Yu, S. Hecht, C. Joachim, L. Grill, *Science* **2009**, *323*, 1193.
[11] D. Zhong, J.-H. Franke, S. K. Podiyanachari, T. Blömker, H. Zhang, G. Kehr, G. Erker, H. Fuchs, L. Chi, *Science* **2011**, *334*, 213.
[12] G. Otero, G. Biddau, C. Sánchez-Sánchez, R. Caillard, M. F. López, C. Rogero, F. J. Palomares, N. Cabello, M. A. Basanta, J. Ortega, J. Méndez, A. M. Echavarren, R. Pérez, B. Gómez-Lor, J. A. Martín-Gago, *Nature* **2008**, *454*, 865.
[13] S. Wang, Q. Sun, O. Gröning, R. Widmer, C. A. Pignedoli, L. Cai, X. Yu, B. Yuan, C. Li, H. Ju, J. Zhu, P. Ruffieux, R. Fasel, W. Xu, *Nat. Chem.* **2019**, *11*, 924.
[14] D. J. Rizzo, G. Veber, T. Cao, C. Bronner, T. Chen, F. Zhao, H. Rodriguez, S. G. Louie, M. F. Crommie, F. R. Fischer, *Nature* **2018**, *560*, 204.
[15] D. J. Rizzo, G. Veber, J. Jiang, R. McCurdy, T. Cao, C. Bronner, T. Chen, S. G. Louie, F. R. Fischer, M. F. Crommie, *Science* **2020**, *369*, 1597.
[16] C. Moreno, M. Vilas-Varela, B. Kretz, A. Garcia-Lekue, M. V. Costache, M. Paradinas, M. Panighel, G. Ceballos, S. O. Valenzuela, D. Peña, A. Mugarza, *Science* **2018**, *360*, 199.
[17] K. Al-Shamery, H.-G. Rubahn, H. Sitter, *Organic Nanostructures for Next Generation Devices*, Springer-Verlag Berlin, Heidelberg, Germany **2008**.
[18] K. Bian, C. Gerber, A. J. Heinrich, D. J. Müller, S. Scheuring, Y. Jiang, *Nat. Rev. Methods Primers* **2021**, *1*, 36.
[19] C. Zhang, Z. Yi, W. Xu, *Mater. Futures* **2022**, *1*, 032301.
[20] C. Zhang, W. Xu, *Aggregate* **2022**, *3*, e175.
[21] L. Dong, Z. A. Gao, N. Lin, *Prog. Surf. Sci.* **2016**, *91*, 101.
[22] D. Écija, J. I. Urgel, A. P. Seitsonen, W. Auwärter, J. V. Barth, *Acc. Chem. Res.* **2018**, *51*, 365.
[23] L. Grill, S. Hecht, *Nat. Chem.* **2020**, *12*, 115.
[24] S. Clair, D. G. de Oteyza, *Chem. Rev.* **2019**, *119*, 4717.
[25] J. Li, X. Wang, Y. He, Z. Xu, X. Li, H. Pan, Y. Wang, Y. Dong, Q. Shen, Y. Zhang, S. Hou, K. Wu, Y. Wang, *J. Phys. Chem. Lett.* **2024**, *15*, 5564.
[26] D. Li, L. Sun, Y. Ding, M. Liu, L. Xie, Y. Liu, L. Shang, Y. Wu, H.-J. Jiang, L. Chi, X. Qiu, W. Xu, *ACS Nano* **2021**, *15*, 16896.

 © 2025 Wiley-VCH GmbH

23669608, 0, Downloaded from https://onlinelibrary.wiley.com/doi/10.1002/smtd.202402118 by Tongji University, Wiley Online Library on [07/04/2025]. See the Terms and Conditions (https://onlinelibrary.wiley.com/terms-and-conditions) on Wiley Online Library for rules of use; OA articles are governed by the applicable Creative Commons License

[27] C. Li, Z. Xu, Y. Zhang, J. Li, N. Xue, R. Li, M. Zhong, T. Wu, Y. Wang, N. Li, Z. Shen, S. Hou, R. Berndt, Y. Wang, S. Gao, *Natl. Sci. Rev.* **2023**, *10*, nwad088.
[28] Y.-Q. Zhang, T. Paintner, R. Hellwig, F. Haag, F. Allegretti, P. Feulner, S. Klyatskaya, M. Ruben, A. P. Seitsonen, J. V. Barth, F. Klappenberger, *J. Am. Chem. Soc.* **2019**, *141*, 5087.
[29] R. Hou, Y. Gao, Y. Guo, C. Zhang, W. Xu, *ACS Nano* **2024**, *18*, 31478.
[30] Z. Zhang, Y. Gao, Z. Yi, C. Zhang, W. Xu, *ACS Nano* **2024**, *18*, 9082.
[31] C. Zhang, L. Xie, L. Wang, H. Kong, Q. Tan, W. Xu, *J. Am. Chem. Soc.* **2015**, *137*, 11795.
[32] M. M. Montemore, M. A. van Spronsen, R. J. Madix, C. M. Friend, *Chem. Rev.* **2018**, *118*, 2816.
[33] J. Quan, F. Muttaqien, T. Kondo, T. Kozarashi, T. Mogi, T. Imabayashi, Y. Hamamoto, K. Inagaki, I. Hamada, Y. Morikawa, J. Nakamura, *Nat. Chem.* **2019**, *11*, 722.
[34] Y.-F. Liang, N. Jiao, *Acc. Chem. Res.* **2017**, *50*, 1640.
[35] S. Santoro, S. I. Kozhushkov, L. Ackermann, L. Vaccaro, *Green Chem.* **2016**, *18*, 3471.
[36] P. Siemsen, R. C. Livingston, F. Diederich, *Angew. Chem., Int. Ed.* **2000**, *39*, 2632.
[37] G. Kyriakou, M. B. Boucher, A. D. Jewell, E. A. Lewis, T. J. Lawton, A. E. Baber, H. L. Tierney, M. Flytzani-Stephanopoulos, E. C. H. Sykes, *Science* **2012**, *335*, 1209.
[38] C. M. Kruppe, J. D. Krooswyk, M. Trenary, *ACS Catal.* **2017**, *7*, 8042.
[39] Y. Wang, H.-X. Lin, L. Chen, S.-Y. Ding, Z.-C. Lei, D.-Y. Liu, X.-Y. Cao, H.-J. Liang, Y.-B. Jiang, Z.-Q. Tian, *Chem. Soc. Rev.* **2014**, *43*, 399.
[40] J. Henzl, K. Boom, K. Morgenstern, *J. Am. Chem. Soc.* **2014**, *136*, 13341.
[41] J. Henzl, K. Boom, K. Morgenstern, *J. Chem. Phys.* **2015**, *142*, 101920.
[42] K. Lucht, I. Trosien, W. Sander, K. Morgenstern, *Angew. Chem., Int. Ed.* **2018**, *57*, 16334.
[43] K. Lucht, D. Loose, M. Ruschmeier, V. Strotkötter, G. Dyker, K. Morgenstern, *Angew. Chem., Int. Ed.* **2018**, *57*, 1266.
[44] C. Zhang, L. Xie, Y. Ding, W. Xu, *Chem. Commun.* **2018**, *54*, 771.
[45] L. Xie, Y. Ding, D. Li, C. Zhang, Y. Wu, L. Sun, M. Liu, X. Qiu, W. Xu, *J. Am. Chem. Soc.* **2022**, *144*, 5023.
[46] C. Zhang, L. Xie, Y. Ding, Q. Sun, W. Xu, *ACS Nano* **2016**, *10*, 3776.
[47] L. Xie, H. Jiang, D. Li, M. Liu, Y. Ding, Y. Liu, X. Li, X. Li, H. Zhang, Z. Hou, Y. Luo, L. Chi, X. Qiu, W. Xu, *ACS Nano* **2020**, *14*, 10680.
[48] K. Yang, L. Liu, L. Zhang, W. Xiao, X. Fei, H. Chen, S. Du, K.-H. Ernst, H.-J. Gao, *ACS Nano* **2014**, *8*, 2246.
[49] M. H. Chang, N.-Y. Kim, Y. H. Chang, Y. Lee, U. S. Jeon, H. Kim, Y.-H. Kim, S.-J. Kahng, *Nanoscale* **2019**, *11*, 8510.
[50] S. Fabris, S. Stepanow, N. Lin, P. Gambardella, A. Dmitriev, J. Honolka, S. Baroni, K. Kern, *Nano Lett.* **2011**, *11*, 5414.
[51] B. E. Murphy, S. A. Krasnikov, N. N. Sergeeva, A. A. Cafolla, A. B. Preobrajenski, A. N. Chaika, O. Lübben, I. V. Shvets, *ACS Nano* **2014**, *8*, 5190.
[52] F. Buchner, K. Seufert, W. Auwärter, D. Heim, J. V. Barth, K. Flechtner, J. M. Gottfried, H.-P. Steinrück, H. Marbach, *ACS Nano* **2009**, *3*, 1789.
[53] K. Seufert, W. Auwärter, J. V. Barth, *J. Am. Chem. Soc.* **2010**, *132*, 18141.
[54] C. Wäckerlin, D. Chylarecka, A. Kleibert, K. Müller, C. Iacovita, F. Nolting, T. A. Jung, N. Ballav, *Nat. Commun.* **2010**, *1*, 61.
[55] T. Knaak, T. G. Gopakumar, B. Schwager, F. Tuczek, R. Robles, N. Lorente, R. Berndt, *J. Am. Chem. Soc.* **2016**, *138*, 7544.
[56] K. Flechtner, A. Kretschmann, H.-P. Steinrück, J. M. Gottfried, *J. Am. Chem. Soc.* **2007**, *129*, 12110.
[57] W. Hieringer, K. Flechtner, A. Kretschmann, K. Seufert, W. Auwärter, J. V. Barth, A. Görling, H.-P. Steinrück, J. M. Gottfried, *J. Am. Chem. Soc.* **2011**, *133*, 6206.
[58] M. Feng, H. Sun, J. Zhao, H. Petek, *ACS Nano* **2014**, *8*, 8644.
[59] M. Feng, H. Petek, Y. Shi, H. Sun, J. Zhao, F. Calaza, M. Sterrer, H.-J. Freund, *ACS Nano* **2015**, *9*, 12124.
[60] C. Bronner, J. Björk, P. Tegeder, *J. Phys. Chem. C* **2015**, *119*, 486.
[61] Z. A. Enderson, H. Murali, R. R. Dasari, Q. Dai, H. Li, T. C. Parker, J.-L. Brédas, S. R. Marder, P. N. First, *ACS Nano* **2023**, *17*, 7366.
[62] R. Zuzak, A. Jančařík, A. Gourdon, M. Szymonski, S. Godlewski, *ACS Nano* **2020**, *14*, 13316.
[63] R. Zuzak, P. Brandimarte, P. Olszowski, I. Izydorczyk, M. Markoulides, B. Such, M. Kolmer, M. Szymonski, A. Garcia-Lekue, D. Sánchez-Portal, A. Gourdon, S. Godlewski, *J. Phys. Chem. Lett.* **2020**, *11*, 10290.
[64] C. Sánchez-Sánchez, J. I. Martínez, N. Ruiz del Arbol, P. Ruffieux, R. Fasel, M. F. López, P. L. de Andres, J. Á. Martín-Gago, *J. Am. Chem. Soc.* **2019**, *141*, 3550.
[65] M. Abyazisani, J. M. MacLeod, J. Lipton-Duffin, *ACS Nano* **2019**, *13*, 9270.
[66] D. Nguyen, G. Kang, N. Chiang, X. Chen, T. Seideman, M. C. Hersam, G. C. Schatz, R. P. Van Duyne, *J. Am. Chem. Soc.* **2018**, *140*, 5948.
[67] D. Grumelli, B. Wurster, S. Stepanow, K. Kern, *Nat. Commun.* **2013**, *4*, 2904.
[68] M. Wang, C. G. Williams, S. L. Tait, *J. Phys. Chem. C* **2019**, *123*, 20980.
[69] P. Ji, G. Galeotti, F. De Marchi, D. Cui, K. Sun, H. Zhang, G. Contini, M. Ebrahimi, O. MacLean, F. Rosei, L. Chi, *Small* **2020**, *16*, 2002393.
[70] P. Ji, O. MacLean, G. Galeotti, D. Dettmann, G. Berti, K. Sun, H. Zhang, F. Rosei, L. Chi, *Sci. China Chem.* **2021**, *64*, 636.
[71] C. Zhang, E. Kazuma, Y. Kim, *J. Am. Chem. Soc.* **2022**, *144*, 10282.
[72] C. Zhang, R. B. Jaculbia, Y. Tanaka, E. Kazuma, H. Imada, N. Hayazawa, A. Muranaka, M. Uchiyama, Y. Kim, *J. Am. Chem. Soc.* **2021**, *143*, 9461.
[73] N. Cao, B. Yang, A. Riss, J. Rosen, J. Björk, J. V. Barth, *Nat. Commun.* **2023**, *14*, 1255.
[74] J. Lawrence, A. Berdonces-Layunta, S. Edalatmanesh, J. Castro-Esteban, T. Wang, A. Jimenez-Martin, B. de la Torre, R. Castrillo-Bodero, P. Angulo-Portugal, M. S. G. Mohammed, A. Matěj, M. Vilas-Varela, F. Schiller, M. Corso, P. Jelínek, D. Peña, D. G. de Oteyza, *Nat. Chem.* **2022**, *14*, 1451.
[75] A. Berdonces-Layunta, J. Lawrence, S. Edalatmanesh, J. Castro-Esteban, T. Wang, M. S. G. Mohammed, L. Colazzo, D. Peña, P. Jelínek, D. G. de Oteyza, *ACS Nano* **2021**, *15*, 5610.
[76] S. Stepanow, N. Lin, J. V. Barth, *J. Phys.: Condens. Matter* **2008**, *20*, 184002.
[77] J. V. Barth, *Surf. Sci.* **2009**, *603*, 1533.
[78] S. O. Parreiras, J. M. Gallego, D. Écija, *Chem. Commun.* **2023**, *59*, 8878.
[79] J. Cai, P. Ruffieux, R. Jaafar, M. Bieri, T. Braun, S. Blankenburg, M. Muoth, A. P. Seitsonen, M. Saleh, X. Feng, K. Müllen, R. Fasel, *Nature* **2010**, *466*, 470.
[80] C. Zhang, E. Kazuma, Y. Kim, *Angew. Chem., Int. Ed.* **2019**, *58*, 17736.
[81] Q. Zhong, K. Niu, L. Chen, H. Zhang, D. Ebeling, J. Björk, K. Müllen, A. Schirmeisen, L. Chi, *J. Am. Chem. Soc.* **2022**, *144*, 8214.
[82] J. Björk, F. Hanke, S. Stafström, *J. Am. Chem. Soc.* **2013**, *135*, 5768.
[83] A. Batra, D. Cvetko, G. Kladnik, O. Adak, C. Cardoso, A. Ferretti, D. Prezzi, E. Molinari, A. Morgante, L. Venkataraman, *Chem. Sci.* **2014**, *5*, 4419.
[84] M. Fritton, D. A. Duncan, P. S. Deimel, A. Rastgoo-Lahrood, F. Allegretti, J. V. Barth, W. M. Heckl, J. Björk, M. Lackinger, *J. Am. Chem. Soc.* **2019**, *141*, 4824.
[85] K. Sun, T. Nishiuchi, K. Sahara, T. Kubo, A. S. Foster, S. Kawai, *J. Phys. Chem. C* **2020**, *124*, 19675.


© 2025 Wiley-VCH GmbH

23669608, 0, Downloaded from https://onlinelibrary.wiley.com/doi/10.1002/smtd.202402118 by Tongji University, Wiley Online Library on [07/04/2025]. See the Terms and Conditions (https://onlinelibrary.wiley.com/terms-and-conditions) on Wiley Online Library for rules of use; OA articles are governed by the applicable Creative Commons License

[86] T. Lin, X. S. Shang, J. Adisoejoso, P. N. Liu, N. Lin, *J. Am. Chem. Soc.* **2013**, *135*, 3576.
[87] J. Adisoejoso, T. Lin, X. S. Shang, K. J. Shi, A. Gupta, P. N. Liu, N. Lin, *Chem. – Eur. J.* **2014**, *20*, 4111.
[88] S. Xing, B. Liu, W. Wang, J. Guo, W. Wang, *Chem. – Asian J.* **2018**, *13*, 2023.
[89] S. Xing, Z. Zhang, X. Fei, W. Zhao, R. Zhang, T. Lin, D. Zhao, H. Ju, H. Xu, J. Fan, J. Zhu, Y.-Q. Ma, Z. Shi, *Nat. Commun.* **2019**, *10*, 70.
[90] B. Cirera, J. Björk, R. Otero, J. M. Gallego, R. Miranda, D. Ecija, *J. Phys. Chem. C* **2017**, *121*, 8033.
[91] L. Xu, C. Zhang, R. Hou, Y. Gao, Z. Zhang, Z. Yi, C. Zhang, W. Xu, *J. Phys. Chem. Lett.* **2024**, *15*, 11862.
[92] R. Hou, Y. Guo, Z. Yi, Z. Zhang, C. Zhang, W. Xu, *J. Phys. Chem. Lett.* **2023**, *14*, 3636.
[93] B. Lowe, J. Hellerstedt, A. Matěj, P. Mutombo, D. Kumar, M. Ondráček, P. Jelinek, A. Schiffrin, *J. Am. Chem. Soc.* **2022**, *144*, 21389.
[94] X. Liu, A. Matej, T. Kratky, J. I. Mendieta-Moreno, S. Günther, P. Mutombo, S. Decurtins, U. Aschauer, J. Repp, P. Jelinek, S.-X. Liu, L. L. Patera, *Angew. Chem., Int. Ed.* **2021**, *61*, 202112798.
[95] X. Zhang, N. Xue, C. Li, N. Li, H. Wang, N. Kocić, S. Beniwal, K. Palotás, R. Li, Q. Xue, S. Maier, S. Hou, Y. Wang, *ACS Nano* **2019**, *13*, 1385.
[96] M. Huš, A. Hellman, *J. Catal.* **2018**, *363*, 18.
[97] J. Wang, K. Niu, H. Zhu, C. Xu, C. Deng, W. Zhao, P. Huang, H. Lin, D. Li, J. Rosen, P. Liu, F. Allegretti, J. V. Barth, B. Yang, J. Björk, Q. Li, L. Chi, *Nat. Commun.* **2024**, *15*, 3030.
[98] L. Xing, J. Li, Y. Bai, Y. Lin, L. Xiao, C. Li, D. Zhao, Y. Wang, Q. Chen, J. Liu, K. Wu, *Nat. Commun.* **2024**, *15*, 666.

**Chi Zhang** received her bachelor and Ph.D. degrees in Engineering from Tongji University (School of Materials Science and Engineering), China in 2012 and 2017 under the supervision of Prof. Wei Xu. Thereafter, she was engaged in the postdoctoral research in RIKEN, Japan from 2018 to 2021 (supervisor: Dr. Yousoo Kim, chief scientist). Since 2021, she started working in the School of Materials Science and Engineering at Tongji University, China as a professor. Her main research interests are on-surface molecular assembly and chemical reactions aiming at fundamental understanding into interfacial chemical processes.

**Rujia Hou** received her bachelor's degree in engineering from Tongji University (School of Materials Science and Engineering), China in 2022. Since 2022, she has been working on the master's degree at the School of Materials Science and Engineering, Tongji University, under the supervision of Prof. Chi Zhang and Prof. Wei Xu. Her research interests include molecular assembly and chemical reactions on metal surfaces under ultrahigh vacuum conditions.

**Wei Xu** received his PhD degree in Science from Aarhus University, Denmark in 2008. Thereafter he was a postdoctoral fellow at Interdisciplinary Nanoscience Center (iNANO), Aarhus University, Denmark and at Departments of Chemistry and Physics, The Penn State University, USA. Since 2009 he has been a full professor at Tongji University, P. R. China. His main research interests are Scanning Tunneling Microscopy (STM) and Density Functional Theory (DFT) investigations of molecular self-assembly and reactions on surfaces under ultrahigh vacuum conditions with the aim of controllably building functional surface nanostructures and gaining fundamental insights into physics and chemistry.


© 2025 Wiley-VCH GmbH

23669608, 0, Downloaded from https://onlinelibrary.wiley.com/doi/10.1002/smtd.202402118 by Tongji University, Wiley Online Library on [07/04/2025]. See the Terms and Conditions (https://onlinelibrary.wiley.com/terms-and-conditions) on Wiley Online Library for rules of use; OA articles are governed by the applicable Creative Commons License